AD_____

Award Number: DAMD17-03-1-0545

TITLE: Engineered Autologous Stromal Cells for the Delivery of Kringle 5, a Potent Endothelial Cell Specific Inhibitor for Anti-Angiogenic Breast Cancer Therapy

PRINCIPLE INVESTIGATOR: Sabrina R. Perri

CONTRACTING ORGANIZATION: S.M.B.D. – Jewish General Hospital
Montreal, Quebec, Canada H3T 1E2

REPORT DATE: August 2006

TYPE OF REPORT: Annual Summary

PREPARED FOR: U.S. Army Medical Research and Materiel Command
Fort Detrick, Maryland 21702-5012

DISTRIBUTION STATEMENT: Approved for Public Release;
Distribution Unlimited

REPORT DOCUMENTATION PAGE

Form Approved
OMB No. 0704-0188

1. REPORT DATE	2. REPORT TYPE	3. DATES COVERED
01-08-2006	Annual Summary	10 Jul 2003 – 9 Jul 2006

4. TITLE AND SUBTITLE

Engineered Autologous Stromal Cells for the Delivery of Kringle 5, a Potent Endothelial Cell Specific Inhibitor for Anti-Angiogenic Breast Cancer Therapy

5a. CONTRACT NUMBER

5b. GRANT NUMBER
DAMD17-03-1-0545

5c. PROGRAM ELEMENT NUMBER

6. AUTHOR(S)

Sabrina R. Perri

5d. PROJECT NUMBER

5e. TASK NUMBER

5f. WORK UNIT NUMBER

7. PERFORMING ORGANIZATION NAME(S) AND ADDRESS(ES)

S.M.B.D. – Jewish General Hospital
Montreal, Quebec, Canada H3T 1E2

8. PERFORMING ORGANIZATION REPORT NUMBER

9. SPONSORING / MONITORING AGENCY NAME(S) AND ADDRESS(ES)
U.S. Army Medical Research and Materiel Command
Fort Detrick, Maryland 21702-5012

10. SPONSOR/MONITOR'S ACRONYM(S)

11. SPONSOR/MONITOR'S REPORT NUMBER(S)

12. DISTRIBUTION / AVAILABILITY STATEMENT
Approved for Public Release; Distribution Unlimited

13. SUPPLEMENTARY NOTES
Original contains colored plates: ALL DTIC reproductions will be in black and white.

14. ABSTRACT

The plasminogen kringle 5 (K5) domain – which is distinct from angiostatin – possesses potent anti-angiogenic properties on its own which can be exploited in cancer therapy. We have previously shown that K5 suppresses cancer growth in tumor xenograft models, its modulation of inflammation in experimental mice with intact immune systems is unknown. To determine whether K5 possesses immune pro-inflammatory properties, we investigated the effects of K5 in an immune competent model of breast cancer and observed that tumor rejection is substantially reduced in NOD-SCID and BALB/c nude when compared to wild-type BALB/c mice, suggesting an important role for T-lymphoid cells in the anti-tumor effect of K5. Tumor explant analysis demonstrates that K5 enhances tumor recruitment of CD3+ lymphoid cells, in particular the NKT phenotype. We also observed a significant decrease in tumor-associated microvessel length and density consistent with anti-angiogenic activity. Histological analysis of K5 tumors also revealed a robust neutrophilic infiltrate, which may be explained by the neutrophil chemotactic activity of K5 as well as its ability to promote CD64 upregulation within the CD11b$^+$ adhesive neutrophil population. In sum, our findings confirm that the K5 protein acts as a potent angiostatic agent and possesses a novel pro-inflammatory role via its ability to recruit tumor-associated neutrophils and NKT-lymphocytes, leading to a potent anti-tumor response.

15. SUBJECT TERMS
Breast Cancer

16. SECURITY CLASSIFICATION OF:			18. NUMBER OF PAGES	19a. NAME OF RESPONSIBLE PERSON USAMRMC
a. REPORT U	**b. ABSTRACT** U	**c. THIS PAGE** U	UU 27	**19b. TELEPHONE NUMBER** *(include area code)*

17. LIMITATION OF ABSTRACT

Standard Form 298 (Rev. 8-98)
Prescribed by ANSI Std. Z39.18

Table of Contents

INTRODUCTION

Proteolytic cleavage products of plasminogen – as well as individual plasminogen kringle domains such as kringle 5 - possess anti-angiogenic properties whose use in cancer therapy is under much scrutiny (1-6). It has been recently proposed that an array of angiostatic agents - including plasminogen derivatives like angiostatin - can significantly stimulate leukocyte-vessel wall interactions *in vivo* by the up-regulation of endothelial adhesion molecules in tumor vessels (7) and may enhance anticancer immune response and allow the immune system to overcome tumor immune resistance (8). However, in the setting of experimental peritonitis, angiostatin has also been shown to behave as an antiadhesive/anti-inflammatory substance (9). The sum of these observations readily supports the anti-angiogenic properties of angiostatin in the setting of pathological neovascularization, but its immune modulatory effects remain controversial. The fifth kringle domain of plasminogen (hereafter K5), when utilized on its own displays robust anti-angiogenic properties (1-3) and will also directly lead to apoptosis of anoxic tumor cells *in vitro* (10). These features make K5 an appealing anti-tumor biopharmaceutical with combined anti-tumoral as well as anti-angiogenic properties. Indeed, we have previously demonstrated that genetic engineering of tumor cells for expression of K5 abolishes tumor growth *in vivo*, potently suppresses cancer-associated angiogenesis and will inhibit recruitment of tumor-associated macrophages in an immune deficient human tumor xenograft model (11). The latter observation suggests that K5 may possess immune modulatory properties on blood-derived immune competent cells – in keeping with the observations made by others with angiostatin. To address the question of K5 influence on immunity, we compared the biology of K5-engineered breast tumor cells in immune defective mice as well as in tumor MHC-matched mice with normal immune systems. As expected, we find that K5 is a potent inhibitor of cancer-associated angiogenesis. However, we also observed that the anti-tumor effect of K5 is utterly dependent on an intact immune system, in particular on the T-lymphocyte subset, and that recruitment of polymorphonuclear cells is a dominant feature of K5 tumors. These observations provide new evidence that the K5 plasminogen derivative possesses anti-angiogenic as well immune stimulatory anti-tumor properties.

BODY (unpublished data)

DA/3 mouse mammary tumor cell line retrovirally engineered to express plasminogen K5 domain.

The human K5 histidine-tagged cDNA (hK5His) was cloned as previously described (11) into a bicistronic retroviral vector construct (14) (Fig. 1*A*). The hK5His retrovector plasmid was stably transfected into 293GPG retroviral packaging cells and retrovirus producer cells were selected as described in Materials and Methods. Tetracycline-withdrawal from the culture media led to the production of VSVG-typed hK5His-GFP retroviral particles which were subsequently concentrated 100-fold by ultracentrifugation and a viral titer of ~2.5×10^6 infectious particles/mL was obtained. Concentrated VSVG-typed hK5His-GFP retroviral particles were utilized to transduce the BALB/c-compatible DA/3 murine mammary cancer cell line. The DA/3 murine mammary adenocarcinoma cell line is estrogen independent and serves as a murine model of locally advanced breast cancer (13, 18-20). Following retroviral transduction, polyclonal gene-modified DA/3 cells were assessed for GFP expression by flow cytometry and sorted to obtain a 100% GFP-positive population. To ensure

hK5His transgene expression and proper secretion, anti-His immunoblot analysis was performed on conditioned supernatant collected from hK5His transduced murine DA/3 mammary tumor cells and detects a major 15kDa protein consistent with the predicted molecular weight of soluble hK5His (Fig. 1*B*). Using a semi-quantitative western blot titration curve, it was estimated that hK5His-GFP-expressing DA/3 cells secrete 0.02pmol/L (or 0.25ng) of soluble hK5His protein per 10^6 cells per 24 hours (data not shown).

Anti-tumor property of hK5His protein is dependent upon an intact immune system.
We tested the efficacy of hK5His against breast cancer in mice with functional immune systems. One million DA/3 (*n* = 10), genetically engineered DA/3-GFP (*n* = 10), or DA/3-hK5His-GFP (*n* = 10) polyclonal cells were implanted subcutaneously in immune competent BALB/c mice and animal survival was monitored over time. One year post-implantation, 65% of hK5His-GFP-implanted mice survived tumor-free (*P* < 0.0001) as compared to 20% in both DA/3- and DA/3-GFP-implanted control mice (Fig. 2*A*). The anti-tumor effect was severely diminished when 10^6 genetically engineered DA/3-GFP (*n* = 10) or DA/3-hK5His-GFP (n = 10) polyclonal cells were implanted subcutaneously in immunodeficient non-obese diabetic severe combined immunodeficient (NOD-SCID) mice (Fig. 2*B*). This mouse strain lacks functional endogenous T or B lymphocytes, due to a deficiency in the recombinase activating gene (RAG)-2 gene, which impairs rearrangement of separate gene elements of the immunoglobulin and T-cell antigen receptor genes and thus disrupts differentiation of both B and T-lymphocyte progenitor cells (21). Although hK5His-GFP-implanted mice succumbed to excessive tumor burden by 2 months post-implantation, their survival was significantly prolonged as compared to control mice (*P* < 0.0001), possibly due to the angiostatic property of hK5His protein. This observation suggests that the immune system is playing a role in the tumoricidal effects of hK5His protein. We proceeded to test whether the immune modulatory effect of hK5His protein was mediated via T lymphocytes by subcutaneously implanting 10^6 DA/3-GFP (*n* = 6) or DA/3-hK5His-GFP (*n* = 6) polyclonal cells in athymic BALB/c nude (T-lymphocyte deficient) mice (Fig. 2*C*). Our results demonstrate that T lymphocytes are required for hK5His protein to exert its anti-tumor action, since all hK5His-GFP-implanted mice had to be sacrificed due to tumor development by 3 months post-implantation, albeit delayed survival compared to GFP-implanted control mice (*P* < 0.0005). In order to assess if hK5His protein elicited an adaptive systemic protective immune response, we subcutaneously implanted wildtype BALB/c mice with irradiated 5 x 10^5 DA/3-GFP (*n* = 10) or DA/3-hK5His-GFP (*n* = 10) cells and 14 days later challenged the mice on the opposite flank with 5 x 10^5 non-irradiated DA/3-GFP cells (Fig. 2*D*). Protective immunity was not observed since there was no significant difference between the survival rate of challenged GFP-implanted and hK5His-GFP-implanted mice (*P* = 0.37).

hK5His protein expression by DA/3 cells leads to recruitment of CD3+ lymphocytes *in vivo*.
To further characterize the immune cellular mediators involved in hK5His protein anti-tumor effect, we embedded 10^6 DA/3-GFP (*n* = 4) or DA/3-hK5His-GFP (*n* = 4) polyclonal cells in Matrigel^{TM} and subcutaneously implanted the cells in immunocompetent BALB/c mice. Implants were retrieved 3 days post-implantation and collagenase-digested to obtain a single cell suspension. Cells in each experimental group were counted using a hemacytometer and the cellular infiltrate was analyzed by staining the single cell suspension with 4-color antibodies enabling the identification of different immune subsets by flow cytometry analysis. Our infiltrate analysis confirms that hK5His protein secreted by gene-engineered DA/3 cells induces a potent host-derived cellular infiltrate including CD45$^+$ hematopoietic cells (Fig. 3*A*). T-lymphoid subset analysis (Fig. 3*B*), demonstrates a

substantial increase in the absolute number of infiltrated CD3$^+$ lymphocytes ($P < 0.005$), in particular CD3$^+$NKT$^+$ cells ($P < 0.05$).

hK5His protein expression by DA/3 cells influences the quantity and size of tumor-associated microvasculature.
We have previously demonstrated that hK5His secretion by human glioma cells leads to a profound anti-angiogenic effect in NOD-SCID mice (11). To test whether this effect was replicated in immune competent BALB/c mice, we embedded 10^6 DA/3 ($n = 4$), DA/3-GFP ($n = 4$) or DA/3-hK5His-GFP ($n = 4$) polyclonal cells in Matrigel^{TM} and subcutaneously implanted the cells in BALB/c mice. One week post-implantation, the Matrigel^{TM} plugs were retrieved (Fig. 4*A*), sectioned and stained with von Willebrand factor (vWF) antibody (Fig. 4*B, left panel*). The number (Fig. 4*C*) as well as the length (Fig. 4*B*, *right panel*) of blood vessels was significantly reduced in the hK5His plugs consistent with a potent anti-angiogenic effect *in vivo*.

hK5His induces neutrophilic tumor infiltration.
In an effort to understand the effect of hK5His on host-derived inflammation, we embedded 10^6 DA/3 ($n = 4$), DA/3-GFP ($n = 4$) or DA/3-hK5His-GFP ($n = 4$) polyclonal cells in Matrigel^{TM} and subcutaneously implanted the cells in immunocompetent BALB/c mice. Implants were retrieved 3 days post-implantation, sectioned, stained with hematoxylin and eosin (H&E) and analyzed by a veterinary pathologist (co-Author: DM). The histological analysis revealed that there were almost no intact islet (acini) of tumor cells in the hK5His-containing implants as compared to the GFP-containing implants (Fig. 5*E*, $P = 0.0001$), where there was a moderate number of islets, sometimes acini, of intact tumor cells present at the periphery of the implants as seen in Fig. 5*A* & *C*. The DA/3-hK5His-GFP tumor cells occurred as single cells, rarely in pairs, in contrast with the DA/3-GFP tumor cells which occurred in islets of at least 6 cells. Most of the DA/3-hK5His-GFP tumor cells observed were either necrotic or degenerated (Fig. 5*D* & *F*) and were often surrounded by inflammatory cells as compared to the DA/3-GFP tumor cells that appeared healthy (no vacuolation, no swelling, no loss of tinctorial affinity, acinar or islet architecture preserved). Both GFP- and hK5His-GFP-containing implants were incompletely surrounded by a capsule at the border regions (Fig. 5*C* & *F* respectively) composed of concentric layers of edematous immature connective tissue (fibroblasts with variable numbers of inflammatory cells). We observed that the hK5His-GFP-containing implants were markedly thickened by a dense population of inflammatory cells (Fig. 5*B* & *D*) composed of at least 50% neutrophils, qualified as suppurative inflammation. Enumeration confirmed a substantial increase in the number of infiltrated neutrophils in the hK5His-GFP-containing implants as compared to the control implants (Fig. 5*E*, $P = 0.0001$). There were several eosinophils in the border zone of both groups. However, there was no significant difference in the number of infiltrated eosinophils between test and control (data not shown).

hK5His protein is chemotactic for neutrophils and promotes their activation.
In order to explain the enhanced recruitment of host-derived neutrophils within the hK5His-GFP-containing implants, we assessed the ability of soluble hK5His protein to act as a neutrophil chemoattractant. PMN isolated from heparinized human peripheral blood were assayed for cell-surface expression of the adhesion marker CD11b (Mac-1) by flow cytometry analysis, and were found to be strongly positive (Fig. 6*A*). PMN were plated on the top surface of the migration filter and exposed to either increasing doses of purified hK5His protein (80, 120 or 160ng) diluted in OPTI-MEM or OPTI-MEM alone as a control. We observed that hK5His protein acts as a potent

neutrophil chemoattractant and displays a dose-response effect (Fig. *6B*). Additionally, we demonstrate that neutrophil exposure to soluble hK5His protein induces increased cell-surface expression of the granulocyte activation marker CD64 (Fcγ receptor I) within the CD11b^{+} (Mac-1) adhesive neutrophil subset (Fig. *6C*). These findings are consistent with our histological analysis and suggest that soluble hK5His protein produced by gene-modified DA/3 cells acts as a strong neutrophil chemoattractant as well as promotes activation of neutrophils within the tumor microenvironment.

MHC I expression in hK5His-expressing DA/3 cells.

MHC I is a key molecule involved in immune surveillance and its level of expression may influence interaction with innate effectors (22-25). Therefore, we ascertained whether hK5His altered this phenotype. We assessed the cell-surface expression of major histocompatibility antigen (MHC) class I on GFP- and hK5His-GFP-expressing DA/3 cells by flow cytometry. Our results indicate that hK5His-GFP-expressing DA/3 cells express similar levels (54.4%) of MHC-I (H-2Kd) molecule as GFP-expressing DA/3 cells (64.1%) ($P > 0.05$) (data not shown).

KEY RESEARCH ACCOMPLISHMENTS

- DA/3 mouse mammary tumor cell line efficiently retrovirally engineered to express human plasminogen K5 domain;
- Anti-tumor property of hK5His protein is dependent upon an intact immune system;
- hK5His protein expression by DA/3 cells leads to recruitment of CD3+ lymphocytes *in vivo;*
- hK5His protein expression by DA/3 cells influences the quantity and size of tumor-associated microvasculature;
- hK5His induces neutrophilic tumor infiltration *in vivo*;
- hK5His protein is chemotactic for neutrophils and promotes their activation and;
- MHC I expression is unchanged in hK5His-expressing DA/3 cells.

REPORTABLE OUTCOMES

Manuscripts

1. The results discussed above were compiled into a manuscript.
   S. R. Perri, D. Martineau, M. François, L. Lejeune, Y. Durocher and J. Galipeau. Plasminogen Kringle 5 blocks tumor progression by anti-angiogenic and pro-inflammatory pathways. *Submitted to Molecular Cancer Therapeutics.*

2. **S. R. Perri,** J. Nalbantoglu, B. Annabi, Z. Koty, L. Lejeune, M. François, M. R. Di Falco, R. Béliveau, and J. Galipeau. Plasminogen Kringle 5-Engineered Glioma Cells Block Migration of Tumor-Associated Macrophages and Suppress Tumor Vascularization and Progression. **Cancer Research** 2005; 65(18) 8359-65.

Abstracts & Invited Presentations

1. **S. R. Perri** and J. Galipeau. <u>Soluble Plasminogen Kringle 5 Protein Enhances Apoptosis of Mammary Adenocarcinoma Cells Under Hypoxia.</u> AACR Proceedings, April 2006.
   This abstract was accepted as a late-breaking abstract for poster presentation at the 97th Annual American Association for Cancer Research Conference in Washington, DC. The 1st author was the recipient of the National Cancer Institute of Canada Senior Ph.D. Travel Award ($1500CAD).

2. **S. R. Perri**, M. François, L. Lejeune, D. Martineau, and J. Galipeau. <u>Human Plasminogen Kringle 5 Protein Domain Acts as a Novel Immunostimulatory and Anti-Angiogenic Biopharmaceutical for Breast Cancer Therapy.</u> September 2005.
   This abstract was accepted for poster presentation at the American Association for Cancer Research Special Conference: Advances in Breast Cancer Research: Genetics, Biology and Clinical Applications in La Jolla, California.

3. **S. R. Perri**, M. François and J. Galipeau. <u>Engineered Murine Mammary Cancer Cells Producing Soluble Human Plasminogen Kringle 5 Peptide Arrest Tumor Growth.</u> Era of Hope Proceedings, June 2005.
   This abstract was accepted for poster presentation at the Era of Hope Department of Defence Breast Cancer Research Program Meeting held in Philadelphia, Pennysylvania.

4. **S. R. Perri**, M. François and J. Galipeau. <u>Human Plasminogen Kringle 5-Engineered Murine Mammary Cancer Cells Arrest Tumor Growth and Promote Long-Term Survival.</u> Molecular Therapy, vol. 11 (supplement 1) June 2005.
   This abstract was accepted for poster presentation at the 8th Annual Meeting of the American Society of Gene Therapy (ASGT) held in St. Louis, Missouri.

5. **S. R. Perri**, B. Annabi, L. Lejeune, M. François, R. Béliveau, J. Galipeau. <u>Soluble Human Plasminogen Kringle 5 Domain Acts as a 2-Pronged Anti-Cancer Agent Inhibiting Both Endothelial and Tumor-Associated Macrophages.</u> AACR Proceedings, April 2005.
   This abstract was accepted for poster presentation at the 96th Annual American Association of Cancer Research (AACR) Meeting held in Anaheim, California.

6. **S. R. Perri**. <u>Plasminogen Kringle 5-Engineered Glioma Cells Block Migration of Tumor-Associated Macrophages and Suppress Tumor Vascularization and Progression.</u> February 11, 2005.
   This abstract was presented as an oral presentation at Molecular Oncology Group Meeting in Montreal, Canada.

7. **S. R. Perri,** J. Nalbantoglu, B. Annabi, Z. Koty, L. Lejeune, M. François, M. R. Di Falco R. Béliveau and J. Galipeau. <u>Gene-Modified Human Glioma Cells Producing Soluble Human Plasminogen Kringle 5 Peptide Suppress Brain Tumor Progression.</u> **Molecular Therapy,** vol. 9 (supplement 1) May 2004.
   *This abstract was accepted for **poster presentation** at the 7th Annual Meeting of the American Society of Gene Therapy (ASGT) held in Minneapolis (June 2004).*

8. **S. R. Perri,** J. Nalbantoglu, B. Annabi, Z. Koty, L. Lejeune, M. François, M. R. Di Falco R. Béliveau and J. Galipeau. <u>Gene-Modified Human Glioma Cells Producing Soluble Human Plasminogen Kringle 5 Peptide Suppress Brain Tumor Progression.</u> May 2004.
*This abstract was awarded the **1st Prize ($500) at the 1st Student Poster Competition at the 2nd Montreal Centre for Experimental Therapeutics in Cancer (MCETC) Meeting** held at the Biotechnology Research Institute.*

9. **S. R. Perri,** J. Galipeau, S. James and M. R. Di Falco. <u>MALDI-QToF Mass   Spectrometry Analysis of Expressed Soluble Kringle 5 Peptide Confirms Expected Disulfide Bridging Conformation.</u> May 2004.
*This abstract was accepted for **poster presentation** at the 4th International Canadian Proteomics Initiative Conference.*

10. **S. R. Perri,** J. Nalbantoglu, B. Annabi, Z. Koty, R. Béliveau and J. Galipeau. <u>Kringle 5, a Novel and Potent Endothelial Cell-Specific Inhibitor for Anti-Angiogenic Gene Therapy of Cancer.</u> November 2003.
*This abstract was **awarded the 1st Prize ($1500) at the 2003 International BioNorth Student Poster Competition** in Ottawa.*

11. **S. R. Perri,** J. Nalbantoglu, B. Annabi, Z. Koty, R. Béliveau and J. Galipeau. <u>Kringle 5, a Novel and Potent Endothelial Cell-Specific Inhibitor for Anti-Angiogenic Gene Therapy of Cancer.</u> October 2003.
*This abstract was **selected among the 12 best submitted abstracts across Canada** to be presented at the 2003 BioContact meeting in Quebec City.*

<u>CONCLUSIONS</u>

We have previously demonstrated that tumor-expressed hK5His leads to a substantial anti-angiogenic effect and cure of human glioma orthotopic xenografts in a majority of athymic *nu/nu* nude mice (11). In the current study, we observed that NOD-SCID and athymic nude BALB/c mice with impaired T-lymphoid immune systems do not mount as effective an anti-tumor response to DA/3 cells expressing hK5His, when compared to immunologically normal rodents. Furthermore, despite apparent long term cures lasting more than 1 year in normal BALB/c mice, we were unable to demonstrate an effective adaptive immune response to tumor challenge, suggesting that components of the innate immune system play an important role in the effectiveness of K5 anti-tumor properties (Fig. 2). These observations are congruent with the hypothesis that anti-angiogenic compounds derived from plasminogen and other sources have pleiotropic effects, which likely involve a synergistic recruitment of an inflammatory anti-tumor response (7, 8). We have observed that tumor expression of hK5His leads to a robust $CD3^+$ lymphoid tumor infiltration, in particular NKT cells, suggesting a role for these immune effector cells in K5-mediated tumor rejection (Fig. 3). Histological examination of tumor implants confirmed a robust suppression of cancer neovascularization (Fig. 4) as well as a marked neutrophilic suppurative reaction (Fig. 5). This neutrophilic infiltration may be mediated by soluble K5 protein, which we demonstrate acts as a chemoattractant for neutrophils and promotes upregulation of the CD64 granulocyte activation marker (Fig. 6). This observation follows in the stead of the recently discovered property of an array of anti-angiogenic pharmaceuticals – including plasminogen derivatives such as angiostatin – to alter

the phenotype of cancer-associated neovasculature in a manner which leads to enhanced tumor recruitment of leukocytes. Dirkx et al., recently reported that a synthetic angiogenesis inhibitor, anginex, enhances leukocyte-vessel wall interactions in tumor vessels by upregulating tumor endothelial VCAM-1 and E-selectin expression, and subsequently increasing infiltration of CD45^{+} leukocytes and cytotoxic CD8^{+} lymphocytes into the tumor to suppress tumor growth (7). Although Dirkx et al., report that angiostatin can also increase the leukocyte-vessel wall interaction in vivo, Chavakis et al., claim that angiostatin acts as an anti-adhesive and anti-inflammatory agent since it inhibits peritonitis-induced neutrophil emigration in vivo via its interaction with α4β1-integrin and Mac-1 (αMβ2-integrin) (9). Our observation that K5 enhances recruitment of NKT cells and neutrophils is in support of a pro-inflammatory mode of action and buttresses the theory that inflammation and microvascular suppression act synergistically in the observed anti-tumor effects of hK5. Our survival data in both immunodeficient NOD-SCID and BALB/c nude mice demonstrates that although host-derived neutrophils may be implicated in suppressing tumor progression, their presence is not sufficient in T-cell deficient mice to eradicate the tumor, suggesting a cooperative anti-tumor effect between these immune effector cells. There is precedence for combined lymphocytic and neutrophilic involvement in tumor rejection. Cairns et al., (26) reported that gene-engineered myeloma cells expressing lymphotactin induced infiltration of CD4^{+}, CD8^{+} and neutrophils leading to effective tumor regression in vivo. Lee et al., (27) described that in vivo injection of IL-8-transfected human ovarian cancer cells induced dramatic neutrophilic infiltration and resulted in decreased tumor growth. In the context of anti-angiogenic therapy, Pike et al., (28) also observed in vivo neutrophilic and lymphocytic infiltration in vasostatin (angiogenic inhibitor)-treated Burkitt lymphoma tumors, which led to tumor suppression.

Work from Abbott Laboratories demonstrates that cancer cells rendered anoxic in vitro translocate GRP78 to the cell membrane which then serves as a ligand for K5. K5-bound GRP78 thereafter initiates an apoptotic cascade (10). The significance of this phenomenon was not tested in experimental animals; however it clearly buttresses the claim that K5 can directly affect the phenotype and cellular function of tumor cells. We did not observe an increased apoptosis index or reduced cell growth of K5-expressing DA/3 cells in standard tissue culture conditions or in a 3% oxygen hypoxic environment, nor were we able to detect membrane-bound GRP78 despite its intracellular abundance in DA/3 cells (data not shown). These observations suggest that K5 likely interacts with tumor cells via a plurality of pathways of which GRP78 may be one in certain circumstances. Thus, it may be speculated that hK5His protein breaks immune tolerance by inducing a cross-talk to occur between host-derived neutrophils and other innate infiltrating immune cells such as NKT-lymphocytes. Furthermore, K5 from DA/3 may lead to an altered adhesive phenotype of tumor-associated vessels and promote local recruitment of leukocytes from blood stream.

In aggregate, our data confirms the anti-angiogenic potency of hK5His and suggests that hK5His protein also relies upon multiple innate cellular effectors to induce its in vivo anti-neoplastic effect. More specifically, our findings demonstrate that hK5His protein requires functional neutrophils and T-lymphocytes in order to induce optimal tumor rejection. Further studies on the pleiotropic effects of K5 protein on vasculature and inflammatory effector cells may provide new insights allowing K5 to be therapeutically exploited to treat cancer.

REFERENCES

1 Cao Y, Ji RW, Davidson D, et al. Kringle domains of human angiostatin. Characterization of the anti-proliferative activity on endothelial cells, J.Biol.Chem., *271:* 29461-29467, 1996.

2 Cao Y, Chen A , An SS, Ji RW, Davidson D, Llinas M. Kringle 5 of plasminogen is a novel inhibitor of endothelial cell growth, J.Biol.Chem., *272:* 22924-22928, 1997.

3 Cao Y, Cao R, Veitonmaki N. Kringle structures and antiangiogenesis, Curr.Med.Chem.Anti.-Canc.Agents, *2:* 667-681, 2002.

4 Chang Y, Mochalkin I, McCance SG, Cheng B, Tulinsky A, Castellino FJ. Structure and ligand binding determinants of the recombinant kringle 5 domain of human plasminogen, Biochemistry, *37:* 3258-3271, 1998.

5 Geiger JH, Cnudde SE. What the structure of angiostatin may tell us about its mechanism of action, J.Thromb.Haemost., *2:* 23-34, 2004.

6 Soff GA. Angiostatin and angiostatin-related proteins, Cancer Metastasis Rev., *19:* 97-107, 2000.

7 Dirkx AE, oude Egbrink MG, Castermans K, et al. Anti-angiogenesis therapy can overcome endothelial cell anergy and promote leukocyte-endothelium interactions and infiltration in tumors, FASEB J., *20:* 621-630, 2006.

8 Sun X, Kanwar JR, Leung E, Lehnert K, Wang D, Krissansen GW. Angiostatin enhances B7.1-mediated cancer immunotherapy independently of effects on vascular endothelial growth factor expression, Cancer Gene Ther., *8:* 719-727, 2001.

9 Chavakis T, Athanasopoulos A, Rhee JS, et al. Angiostatin is a novel anti-inflammatory factor by inhibiting leukocyte recruitment, Blood, *105:* 1036-1043, 2005.

10 Davidson DJ, Haskell C, Majest S, et al. Kringle 5 of human plasminogen induces apoptosis of endothelial and tumor cells through surface-expressed glucose-regulated protein 78, Cancer Res., *65:* 4663-4672, 2005.

11 Perri SR, Nalbantoglu J, Annabi B, et al. Plasminogen kringle 5-engineered glioma cells block migration of tumor-associated macrophages and suppress tumor vascularization and progression, Cancer Res., *65:* 8359-8365, 2005.

12 Ory DS, Neugeboren BA, Mulligan RC. A stable human-derived packaging cell line for production of high titer retrovirus/vesicular stomatitis virus G pseudotypes, Proc.Natl.Acad.Sci.U.S.A, *93:* 11400-11406, 1996.

13 Medina D. Mammary tumorigenesis in chemical carcinogen-treated mice. VI. Tumor-producing capabilities of mammary dysplasias in BALB/cCrgl mice, J.Natl.Cancer Inst., *57:* 1185-1189, 1976.

14 Galipeau J, Li H, Paquin A, Sicilia F, Karpati G, Nalbantoglu J. Vesicular stomatitis virus G pseudotyped retrovector mediates effective in vivo suicide gene delivery in experimental brain cancer, Cancer Res., 59: 2384-2394, 1999.

15 Eliopoulos N, Galipeau J. Green Fluorescent Protein. In: B.W.Hicks (ed.), pp. 353-371. Humana Press Inc.: Totowa, 2002.

16 Stagg J, Lejeune L, Paquin A, Galipeau J. Marrow stromal cells for interleukin-2 delivery in cancer immunotherapy, Hum.Gene Ther., 15: 597-608, 2004.

17 Frevert CW, Wong VA, Goodman RB, Goodwin R, Martin TR. Rapid fluorescence-based measurement of neutrophil migration in vitro, J.Immunol.Methods, 213: 41-52, 1998.

18 Matory YL, Chen M, Goedegebuure PS, Eberlein TJ. Anti-tumor effects and tumor immunogenicity following IL2 or IL4 cytokine gene transfection of three mouse mammary tumors, Ann.Surg.Oncol., 2: 502-511, 1995.

19 Matory YL, Chen M, Dorfman DM, Williams A, Goedegebuure PS, Eberlein TJ, Antitumor activity of three mouse mammary cancer cell lines after interferon-gamma gene transfection, Surgery, 118: 251-255, 1995.

20 Baruch A, Hartmann M, Zrihan-Licht S, et al. Preferential expression of novel MUC1 tumor antigen isoforms in human epithelial tumors and their tumor-potentiating function, Int.J.Cancer, 71: 741-749, 1997.

21 Prochazka M, Gaskins HR, Shultz LD, Leiter, EH. The nonobese diabetic scid mouse: model for spontaneous thymomagenesis associated with immunodeficiency, Proc.Natl.Acad.Sci.U.S.A, 89: 3290-3294, 1992.

22 Karre K. NK cells, MHC class I molecules and the missing self, Scand.J.Immunol., 55: 221-228, 2002.

23 Levitsky HI, Lazenby A, Hayashi RJ, Pardoll DM. In vivo priming of two distinct antitumor effector populations: the role of MHC class I expression, J.Exp.Med., 179: 1215-1224, 1994.

24 Moron G, Dadaglio G, Leclerc C. New tools for antigen delivery to the MHC class I pathway, Trends Immunol., 25: 92-97, 2004.

25 Trombetta ES, Mellman I. Cell biology of antigen processing in vitro and in vivo, Annu.Rev.Immunol., 23: 975-1028, 2005.

26 Cairns CM, Gordon JR, Li F, Baca-Estrada ME, Moyana T, Xiang J. Lymphotactin expression by engineered myeloma cells drives tumor regression: mediation by CD4+ and CD8+ T cells and neutrophils expressing XCR1 receptor, J.Immunol., 167: 57-65, 2001.

27 Lee LF, Hellendall RP, Wang Y, et al. IL-8 reduced tumorigenicity of human ovarian cancer in vivo due to neutrophil infiltration, J.Immunol., 164: 2769-2775, 2000.

28 Pike SE, Yao L, Jones KD, et al. Vasostatin, a calreticulin fragment, inhibits angiogenesis and suppresses tumor growth, J.Exp.Med., 188: 2349-2356, 1998.

APPENDICES

Plasminogen Kringle 5–Engineered Glioma Cells Block Migration of Tumor-Associated Macrophages and Suppress Tumor Vascularization and Progression

Sabrina R. Perri,[1,2] Josephine Nalbantoglu,[3] Borhane Annabi,[6] Zafiro Koty,[4] Laurence Lejeune,[2] Moïra François,[2] Marcos R. Di Falco,[5] Richard Béliveau,[7] and Jacques Galipeau[1,2,8]

[1]Division of Experimental Medicine, [2]Lady Davis Institute for Medical Research; [3]Department of Neurology and Neuroscience, [4]Montreal Neurological Institute, McGill University; [5]McGill University and Genome Quebec Innovation Centre; [6]Department of Biochemistry, [7]Laboratoire de Médecine Moléculaire, Centre de Cancérologie Charles-Bruneau, Hôpital Sainte-Justine, Université de Québec à Montréal; and [8]Division of Hematology/Oncology, Department of Medicine, Jewish General Hospital, Montreal, Quebec, Canada

Abstract

Angiostatin, a well-characterized angiostatic agent, is a proteolytic cleavage product of human plasminogen encompassing the first four kringle structures. The fifth kringle domain (K5) of human plasminogen is distinct from angiostatin and has been shown, on its own, to act as a potent endothelial cell inhibitor. We propose that tumor-targeted K5 cDNA expression may act as an effective therapeutic intervention as part of a cancer gene therapy strategy. In this study, we provide evidence that eukaryotically expressed His-tagged human K5 cDNA (hK5His) is exported extracellularly and maintains predicted disulfide bridging conformation in solution. Functionally, hK5His protein produced by retrovirally engineered human U87MG glioma cells suppresses *in vitro* migration of both human umbilical vein endothelial cells and human macrophages. Subcutaneous implantation of Matrigel-embedded hK5His-producing glioma cells in non-obese diabetic/severe combined immunodeficient mice reveals that hK5His induces a marked reduction in blood vessel formation and significantly suppresses the recruitment of tumor-infiltrating CD45$^+$Mac3$^+$Gr1$^-$ macrophages. Therapeutically, we show in a nude mouse orthotopic brain cancer model that tumor-targeted K5 expression is capable of effectively suppressing glioma growth and promotes significant long-term survival (>120 days) of test animals. These data suggest that plasminogen K5 acts as a novel two-pronged anticancer agent, mediating its inhibitory effect via its action on host-derived endothelial cells and tumor-associated macrophages, resulting in a potent, clinically relevant antitumor effect. (Cancer Res 2005; 65(18): 8359-65)

Introduction

Glioblastomas are very aggressive solid tumors characterized by hypervascularization and extensive tumor cell invasion into normal brain parenchyma (1). Current therapeutic modalities primarily target rapidly dividing malignant cells and include combinations of surgery, radiotherapy, and chemotherapy (1, 2). However, these therapies remain ineffective with >90% of patients experiencing local recurrence and a 5-year survival rate of only 9% (3).

The urgent need for the development of potent antiglioma therapeutics as well as the importance of angiogenesis in glioma growth (4, 5) has fueled the identification and characterization of numerous antiangiogenic agents, aimed at interrupting new vessel formation and ultimately arresting tumor growth. The use of antiangiogenic agents as therapeutics is an appealing approach targeting nonmalignant endothelial cells that form the tumor vasculature and indirectly affects tumor cells thus minimizing the risk of toxicity. In addition, the problem of drug resistance associated with conventional chemotherapy agents is avoided because normal endothelial cells are genetically stable unlike tumor cells (6). Moreover, the blood-brain barrier is another obstacle often encountered with therapies targeting malignant cells within the brain and may be exploited with antiangiogenic strategies by maintaining the angiogenic inhibitor within the brain vasculature for a prolonged period. Although angiogenesis inhibition offers several advantages over traditional therapeutic approaches, it is expected to induce a cytostatic effect resulting in tumor stabilization not eradication. Furthermore, single-agent antiangiogenic therapy may lead to a compensatory increase in the production of other angiogenic factors, which may then sustain angiogenesis (1). Despite these limitations, it is now well recognized that angiostatic agents either singly or in combination with other treatment modalities could offer superior therapeutic benefits than currently attainable (7–13), converting the tumor into a controlled, quiescent chronic disease. Direct delivery of purified recombinant antiangiogenic proteins however necessitates large quantities and repeated administration of the therapeutic gene product for a prolonged period of time (14, 15). To circumvent the pitfalls associated with conventional treatments, we have developed a potent antiangiogenic gene therapy strategy for brain cancer. Moreover, because malignant gliomas localize within the central nervous system and do not form distant metastases (16), they represent an attractive target for local gene therapy, which provides high and sustained local production of the desired therapeutic agent and offers a viable alternative to existing therapeutic interventions.

Several inhibitors of angiogenesis exist endogenously as proteolytic cleavage products of larger precursor molecules. Angiostatin, a well-characterized antiangiogenic agent discovered by O'Reilly et al. in Folkman's laboratory, was initially identified as an endothelial cell growth inhibitor present in urine and plasma of animals harboring solid tumors (17, 18), is an internal cryptic fragment of human plasminogen encompassing the first four kringle (K1-4) domains (Fig. 1A). The K5 domain of plasminogen has been

expressed as a recombinant protein in bacteria and been found to be more potent than K1-4 or any of the plasminogen kringles expressed individually in inhibiting growth factor stimulated proliferation of endothelial cells *in vitro* (19, 20). It has also been shown that kringle domains 1-5 (K1-5) act as more potent endothelial cell inhibitors *in vitro* and are more effective in suppressing fibrosarcoma tumor growth *in vivo* compared with K1-4 alone (21). We propose that the K5 domain could serve as a potent angiostatic agent on its own and that it may act as a useful therapeutic transgene within a cancer gene therapy strategy. To test this hypothesis, we have developed a human K5-expressing retroviral vector and tested its efficacy *in vivo* using an orthotopic brain cancer model.

Materials and Methods

Cell culture reagents. 293GPG pantropic retrovirus-packaging cell line (22) was a gift from Dr. Richard C. Mulligan (Children's Hospital, Boston, MA). Human glioma U87MG cell line (23) was a gift from Dr. Stéphane Richard (Lady Davis Institute, Montreal, Quebec, Canada). Freshly isolated primary human umbilical endothelial cells (HUVEC) were generously provided by Dr. Mark Blostein (Lady Davis Institute) and maintained in endothelial-basal media (EBM-2; Cambrex, Walkersville, MD) supplemented with EBM-2 SingleQuots. Fresh human peripheral blood mononuclear cells were obtained from normal volunteers and maintained in DMEM-F12 (Wisent Technologies, St-Bruno, QC, Canada) supplemented with 2%

human serum and 500 units/mL granulocyte/macrophage colony stimulating factor (GM-CSF; Immunex, Thousand Oaks, CA).

Soluble human kringle 5-hisTag expression vector, protein purification, and detection. pBLAST-hK5 cDNA (InvivoGen, San Diego, CA) encodes for hK5 and contains a 5′ interleukin-2 signal peptide (IL-2sp) coding sequence. A 3′ 6-histidine tag was PCR cloned to generate IL-2sp/hK5/HisTag (hereafter hK5His). Conditioned medium was collected from hK5His stably transfected human kidney 293 T cells, concentrated using a Centricon Plus-20 column (Millipore, Billerica, MA) and purified using a Ni-NTA-based resin affinity chromatography purification system (Novagen, San Diego, CA). Immunoblot analysis was done on eluted fractions using a polyclonal anti-His antibody (Santa Cruz Biotechnology, Santa Cruz, CA).

Proteomic analysis of purified soluble hK5His. Lyophilized hK5His samples were resuspended in water/5% acetonitrile/0.1% trifluoroacetic acid (TFA), desalted using reverse-phase C18 ZipTips (Millipore), eluted with water/70% acetonitrile/0.1% TFA. The eluate was spotted onto a matrix-assisted laser desorption ionization (MALDI) sample plate and analyzed using a MALDI time-of-flight (TOF) Voyager-DE (Applied Biosystems, Foster City, CA). The eluted fraction was also spotted onto polybrene-coated TFA filter discs for Edman degradation-based NH₂-terminal sequence analysis using a Procise 492 automated microsequencer (Applied Biosystems). One eluate aliquot was treated with 10 mmol/L DTT for 1 hour, diluted with 80 µL of 50 mmol/L Ambic containing 100 ng of Trypsin gold (Promega, Madison, WI), and digested overnight. For dual-enzyme digest, the eluted fraction was first digested overnight with immobilized trypsin (Pierce, Rockford, IL) followed by an overnight digestion with 100 ng of Endoproteinase-Asp-N (Roche Diagnostics, Laval, Quebec, Canada). Digested solutions were ziptipped and eluted onto a MALDI sample plate. Peptide fragment analysis was done with an Ultima MALDI-Quadrupole TOF mass spectrometer (Waters Limitée, Dorval, Quebec, Canada). Spectra analysis and peptide identity assignment was done using Biolynx, a software tool of Masslynx v4.0 (Waters).

VSV-G-pseudotyped retroviral vector design, synthesis, and titer assessment. The bicistronic murine retrovector pIRES-EGFP was previously generated in our laboratory (24) and contains an enhanced green fluorescent protein (EGFP). The hK5His cDNA was ligated into pIRES-EGFP to generate phK5His-IRES-EGFP. VSV-G-pseudotyped retroparticles encoding hK5His-IRES-EGFP were generated by tetracycline withdrawal as previously published (24, 25). Engineered retroparticles were devoid of replication-competent retrovirus as determined by GFP marker rescue assay using conditioned medium from target cells. The titer of the control GFP and hK5His 293GPG single clone population was assessed as previously described (25).

Transduction of human U87MG glioma cells. Glioma cells were transduced with hK5His-expressing retroviral particles as previously described (24). Stably transduced glioma cells were culture expanded and sorted to obtain both polyclonal and single clone populations based on GFP expression using a Becton Dickinson FACSTAR sorter.

Western blot analysis. Conditioned medium was collected from confluent control GFP and hK5His-transduced U87 glioma cells, as well as stably transfected hK5His 293 T cells (positive control), concentrated, and detected by anti-His immunoblot analysis as previously mentioned.

Migration assays. HUVEC (1×10^4) or human macrophages (5×10^4) were plated onto 0.15% gelatin/PBS-coated 8-µm pore chemotaxis membranes (Corning, Acton, MA) within Boyden chamber inserts. Migration assays were done as previously described (26). HUVEC and macrophages were exposed to conditioned medium from control GFP and hK5His transduced U87 glioma cells for 4 and 24 hours, respectively, under growth factor–stimulated conditions (EBM-2 SingleQuots) and serum stimulation, respectively. Each sample was tested in triplicate and the average number of migrating cells per field was assessed by counting three random high-power fields per filter.

***In vivo* Matrigel assay and analysis of cellular infiltrate by cytometry.** Culture-expanded U87-GFP and U87-hK5His-GFP cells were aliquoted to create 50-µL cell suspensions containing 2×10^4 cells, mixed with 500 µL Matrigel (BD Biosciences, San Jose, CA) at 4°C, and implanted s.c. in the right lateral flank of 6-week-old nonobese diabetic/severe
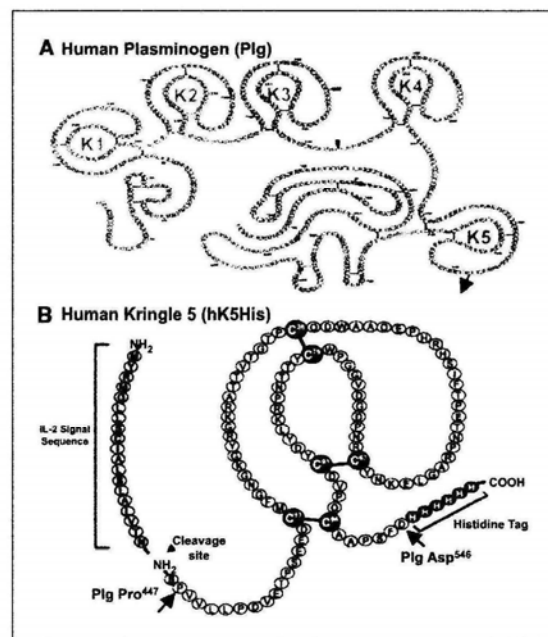
Figure 1. Schematic illustration of human plasminogen (*Plg*) and its kringle domains. *A*, plasminogen is composed of 791 amino acids with a single N-linked glycosylation at Asn²⁸⁹ and a single O-linked glycosylation at Thr³⁴⁶. Angiostatin, a well-known inhibitor of angiogenesis, encompasses the first three to four kringle structures of plasminogen. This is a modified schematic courtesy of Dr. M.R. Llinás et al., Carnegie Mellon University, Pittsburgh, PA (http://www.chem.cmu.edu/groups/Llinas/res/structure/hpk.html). *B*, hK5 consists of the last cryptic fragment of plasminogen (Cys⁴⁶²-Cys⁵⁴¹) and is composed of 80-amino-acid residues with three distinct disulfide bonds.

combined immunodeficient (NOD-SCID) mice (Charles River, Laprairie, Quebec, Canada). Four weeks after implantation, mice were sacrificed and implants excised and processed as previously described (27). To determine the explant cellular infiltrate, cell suspensions were stained with the following antibodies: purified rat anti-mouse CD16/CD32 (mouse Fc block) followed by APC-conjugated rat anti-mouse CD45, PE-conjugated rat anti-mouse Mac-3, biotin-conjugated rat anti-mouse Ly-6G (Gr-1), and their corresponding isotypic controls. Biotinylated antibodies were revealed using PE-Cy7-streptavidin (BD PharMingen, San Diego, CA). Cells were fixed with 1% paraformaldehyde and events were acquired using a FACSCalibur flow cytometer (Beckman Coulter, Fullerton, CA) and analyzed using the CellQuest software (BD PharMingen).

Matrigel explant histochemistry. Explants were fixed in formalin, embedded in paraffin, and 4-μm sections were prepared to generate representative sections of the border and central regions of the explants. Sections were treated with xylene, rehydrated, and antigen retrieval was done using two microwave boils in a 10 mmol/L sodium citrate buffer (pH 6.0) solution. Endogenous biotin activity was blocked using a kit (Zymed Laboratories, Markham, Ontario, Canada), sections were subsequently blocked with 2.5% bovine serum albumin in PBS and incubated with a rabbit polyclonal raised against murine von Willebrand factor (vWF; Neomarkers, Fremont, CA dilution 1:100) overnight. After three washes, the sections were incubated with biotinylated goat anti-rabbit IgG antibody (BD PharMingen, dilution 1:200) for 2 hours, washed, and incubated with streptavidin-peroxidase (Vector Labs, Burlingame, CA) for 1 hour before the addition of 3,3′-diaminobenzidine chromogenic substrate (Vector Labs). Meyer's hematoxylin was used for counterstaining. The blood vessel surface area of all vWF-positive vessels was calculated using a Leica light microscope ocular micrometer (Leica Microsystems, Inc., Richmond Hill, Ontario, Canada) at 400× magnification. Two observers counted three random sections per explant in each experimental group. The blood vessel surface area to total section surface area was calculated and expressed as a percentage.

Stereotactic intracerebral surgery. CD1 *nu/nu* female 6-week-old athymic nude mice (Charles River) were anesthetized using a ketamine/xylezine/saline/acepromazine cocktail (100 mg/mL, 20 mg/mL, 0.9%, 10 mg/mL, respectively) dosed at 100 μL/100 g by i.p. injection. Mice were secured in stereotactic apparatus (Kopf Instruments, Tujunga, CA) and incisor bar set to −1.5. Midline incision made on scalp to expose Bregma and Lambda. Coordinates from Bregma were AP, +0.5; LM, −2.0; and DV, −4.4. A burr hole was made and a Hamilton syringe (10-μL 26-gauge needle, Hamilton Co., Reno, NV) was gently lowered. Cell suspension (1×10^5 in 3 μL of HBSS) was injected at a rate of 0.25 μL per 3 minutes for 36 minutes.

Brain tissue analysis. After euthanasia, brains were processed for H&E staining as previously described (28). Digital images were retrieved using an Olympus microscope (Olympus America, Melville, NY). Tumor volumes were calculated using the formula, length $\times$ width^2 $\times$ 0.4.

Results

Matrix-assisted laser desorption ionization-quadrupole time-of-flight mass spectrometry analysis of expressed soluble hK5His peptide confirms predicted disulfide bridging conformation. The 381-bp human plasminogen K5 domain cDNA, corresponding to amino acid residues 447 to 546 of plasminogen, includes a 20-amino-acid IL-2 signal sequence and a His-tag at the COOH terminus (Fig. 1*B*) and encodes for the hK5His protein with a kringle structure as predicted by previously published nuclear magnetic resonance (NMR) structure study (29). Affinity chromatography was done on precleared conditioned medium from stably transfected hK5His-expressing 293T cells. Anti-His immunoblot, following SDS-PAGE separation (Fig. 2*A, top*), shows a major band of 15 kDa (Fig. 2*A, bottom*). NH$_2$-terminal amino acid sequencing indicated proper cleavage of the IL-2 signal sequence directly upstream of Ser^{20} and analysis by MALDI-Q TOF mass spectrometry revealed a major peak at 12,108 Da consistent with the

predicted molecular weight of hK5His (Fig. 2*B*). To fully characterize cystinyl bridge structure and confirm kringle domain tertiary structure, an orthogonal digestion was carried out either with agarose-immobilized trypsin alone (Fig. 2*C*) or with trypsin followed by incubation with Asp-N endopeptidase (Fig. 2*D*) under reducing and nonreducing conditions. Peptide mapping of non-reduced single and dual protease hK5His digests by MALDI-Q TOF mass spectrometry confirmed the presence of disulfide bridges among Cys^{17}-Cys^{96}, Cys^{38}-Cys^{79}, and Cys^{67}-Cys^{91} (by deduction). These findings show that plasminogen hK5His domain spontaneously adopts a tertiary structure consistent with native conformation as displayed within plasminogen when expressed by genetically engineered eukaryotic cells.

hK5His protein secreted by retrovirally gene-modified human glioma cells inhibits *in vitro* endothelial cell migration. The hK5His cDNA was cloned into our previously published (24) bicistronic retroviral vector (Fig. 3*A*). The hK5His retrovector plasmid was stably transfected into 293GPG retroviral packaging
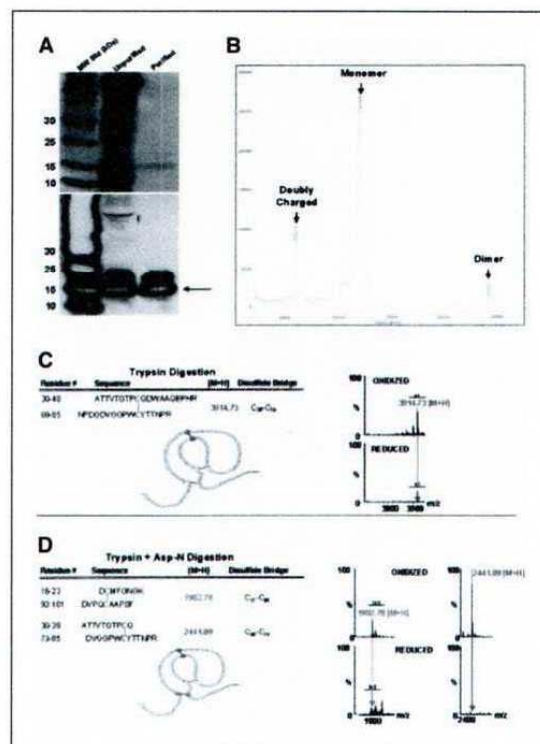
Figure 2. Proteomic analysis of purified soluble hK5His. *A*, silver stain done on pooled eluted fractions detects purified protein at the expected molecular weight of 15 kDa (*top*). Anti-His immunoblot analysis demonstrates the presence of soluble hK5His peptide in pooled eluted fractions (*bottom*). *B*, analysis of the purified hK5His peptide by MALDI-Q TOF mass spectrometry revealed a major peak at 12,108 Da consistent with the theoretical molecular weight of monomeric K5 at 12,109.6 Da. The doubly charged form and dimer are detectable at 6,059 and 24,195 Da, respectively. *C*, expected peptide fragment of interest generated for hK5His protein digested with trypsin alone under oxidizing conditions (*left*). *C*, MALDI-Q TOF mass spectra confirming Cys$^{38:79}$ disulfide bond within hK5His (*right*). *D*, expected peptide fragment of interest generated for hK5His protein digested with trypsin followed by Asp-N endopeptidase treatment under oxidizing conditions (*left*). Spectra confirming Cys$^{17:96}$ and Cys$^{38:79}$ disulfide bonds (*right*).
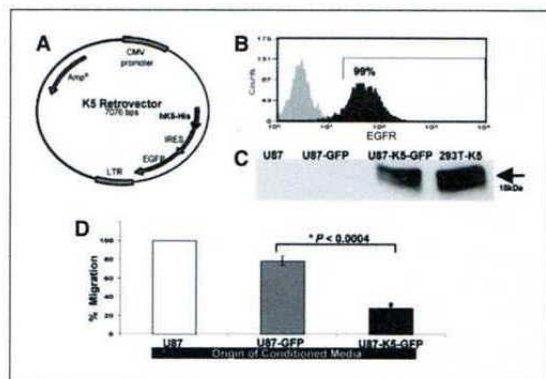
Figure 3. Development and characterization of hK5His-GFP gene-modified cells. *A,* schematic illustration of the human hK5His-IRES-EGFP retroviral plasmid construct. The retrovector pIRES-EGFP construct served as the control plasmid. *B,* flow cytometry analysis of untransduced (*gray*) and hK5His-transduced (*black*) human U87 glioma cells. *C,* anti-His immunoblot analysis reveals functional secretion of hK5His migrating as a doublet at ~15 kDa from retrovirally gene-modified U87 glioma cells and stably transfected 293T cells (positive control). *D,* conditioned medium from hK5His-transduced glioma cells inhibits HUVEC migration up to 75 ± 3%. *Bars,* SE. Statistical analysis was done using Student's *t* test.

cells and retrovirus producer cells were selected as described in Materials and Methods. Tetracycline withdrawal from the culture medium led to the production of VSV-G-typed hK5His-GFP retroviral particles that were subsequently concentrated 100-fold by ultracentrifugation and a viral titer of ~2.5 × 10^6 infectious particles/mL was obtained (data not shown). Concentrated VSV-G-typed hK5His-GFP retroviral particles were used to transduce human glioma cells. The U87MG human glioblastoma cell line was selected for this study because it overexpresses vascular endothelial growth factor (VEGF)–producing tumors *in vivo* that are characterized by increased vascularity, lack of necrosis, and absence of peripheral invasion in early tumor development (1). Following retroviral transduction, single U87MG clones were selected and assessed for GFP expression by flow cytometry. The U87 single clone used for the study was sorted based on GFP expression and was 99% GFP positive (Fig. 3*B*). To ensure hK5His transgene expression and proper secretion, anti-His immunoblot analysis was done on conditioned supernatant collected from hK5His transduced human U87 glioma cells and detects a major 15-kDa protein consistent with the predicted molecular weight of soluble hK5His (Fig. 3*C*). Using a semiquantitative Western blot titration curve, it was estimated that hK5His-GFP-expressing U87 cells secrete 0.5 pmol/L (or 7.5 ng) of soluble hK5His per 10^6 cells per 24 hours (data not shown). To test the functionality of secreted hK5His from hK5His-GFP-expressing U87 cells, a HUVEC migration assay was done as it has been previously shown that recombinant K5 protein is capable of inhibiting the migration of bovine capillary endothelial cells (30). Soluble hK5His present in the conditioned medium of hK5His-GFP-expressing U87 cells was capable of inhibiting growth factor–induced migration of HUVEC up to 75 ± 3% (*P* < 0.0004) compared with conditioned medium from GFP-expressing U87 cells (Fig. 3*D*). This confirms the *in vitro* functionality of hK5His secreted by hK5His-GFP-expressing U87 cells.

hK5His blocks glioma-associated angiogenesis and possesses novel antimacrophage properties. To further characterize the mechanism of action of soluble hK5His *in vivo*, we investigated

whether hK5His could interfere with the tumor microenvironment. More specifically, we assessed whether soluble hK5His could affect the recruitment of host-derived tumor-infiltrating endothelial as well as inflammatory cells implicated in tumor angiogenesis. To test this hypothesis, 2 × 10^4 U87-GFP (*n* = 10) or U87-hK5His-GFP (*n* = 10) cells were Matrigel embedded and implanted s.c. in NOD-SCID mice. To verify if tumor-secreted hK5His induced an antiangiogenic effect *in vivo*, explants (*n* = 4) in each experimental group were retrieved 4 weeks after implantation (Fig. 4*A*) and stained with vWF antibody (Fig. 4*B*). The section surface area occupied by vWF-positive blood vessels to total section surface
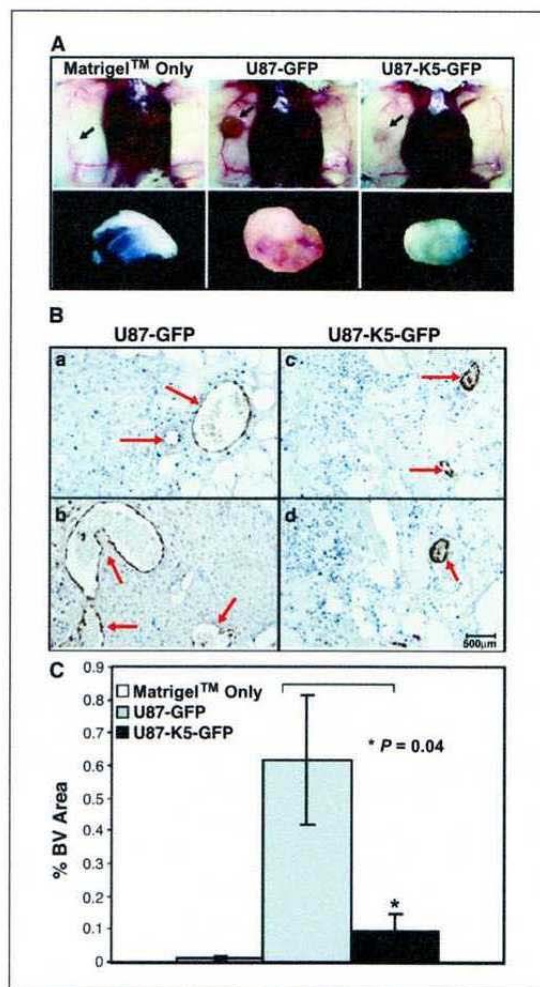
Figure 4. hK5His acts as a potent antiangiogenic agent. *A,* implant (*arrow*) retrieval 4 weeks after implantation of 2 × 10^4 Matrigel-embedded U87-GFP or U87-hK5His-GFP cells (representative images are shown at the same magnification). *B,* representative images of vWF-positive immunostained blood vessels (*red arrows*) from two different U87-GFP-containing (*a* and *b*) and U87-hK5His-GFP-containing (*c* and *d*) implants; magnification, 200×. *C,* vWF-positive blood vessel surface area to total section surface area ratio is plotted as a percentage. *Bars,* SE (SE for Matrigel-only group was based on three random section counts from one animal because remaining implants resorbed completely). Statistical analysis was done using Student's *t* test.

area ratio was calculated and expressed as a percentage (Fig. 4C). Our results show that soluble hK5His domain is capable of exerting a potent antiangiogenic effect ($P = 0.04$) *in vivo* when secreted by retrovirally engineered glioma cells. The remaining explants ($n = 6$) in each experimental group were dissolved in a collagenase solution and single-cell suspensions were generated and counted. (Fig. 5A, *left*). The hK5His-GFP explants contained about two thirds less cells than the control GFP explants ($P = 0.01$). The cellular infiltrate in the explants was analyzed for GFP expression as well as for cell surface marker expression to distinguish the various cell types present within the explants (Fig. 5A, *right*). The GFP-positive cell fraction representing glioma cells is significantly reduced in the hK5His-GFP explants compared with the control GFP explants
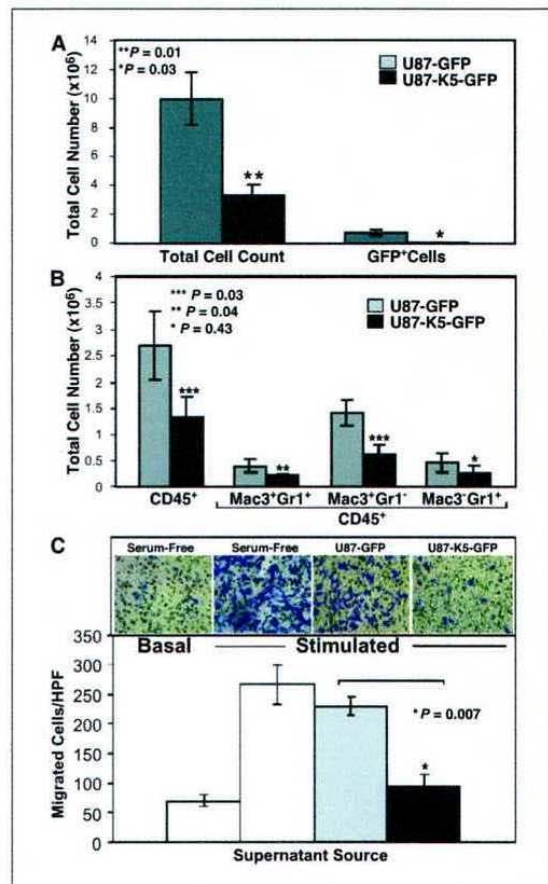
Figure 5. hK5His possesses novel antimacrophage property and decreases migration potential of human macrophages. *A*, absolute total cell count performed after collagenase digestion of the explants (*left*). Absolute number of GFP positive cells was enumerated using flow cytometry and represents the GFP-marked glioma cells (*right*). Bars, SE. *B*, absolute number of infiltrated CD45$^+$ hematopoietic cells, CD45$^+$Mac3$^+$Gr1$^+$ monocytes/macrophages, CD45$^+$Mac3$^+$Gr1$^-$ macrophages and CD45$^+$Mac3$^-$Gr1$^+$ granulocytes in the explants. *Bars*, SE. Statistical analysis was done using Student's *t* test. *C*, macrophages were exposed to various conditioned medium for 24 hours under serum stimulation. Basal invasion represents migrating macrophages under serum-free conditions. *Bars*, SE. *Insets*, representative stains of migrated cells from each experimental group; magnification, 200×. Statistical analysis was done using Student's *t* test.

($P = 0.03$). It is important to note that the difference in absolute tumor cell number is not due to differences in the proliferation rates of the control GFP and hK5His-GFP glioma cells because both possess equivalent proliferation rates *in vitro* (Supplementary Fig. 1). Although immunocompromised NOD-SCID mice possess functional macrophages and granulocytes, they lack functional T and B lymphocytes. Flow cytometry analysis after three-color staining indicated that a substantial part of the cellular infiltrate consisted of CD45-positive hematopoietic cells (Fig. 5B, *left*). More specifically, there was a reduced absolute number of recruited CD45$^+$Mac$^+$Gr1$^+$ ($P = 0.04$) cells, which represents the monocyte/macrophage fraction and CD45$^+$Mac3$^+$Gr1$^-$ ($P = 0.03$) cells, which represents the macrophages present in the U87-hK5His-GFP-containing explants compared with the control U87-GFP-containing explants (Fig. 5B). There was no significant difference in the number of CD45$^+$Mac3$^-$Gr1$^+$ ($P = 0.43$) cells representing the infiltrated granulocytes present in the explants.

To confirm our *in vivo* observations, we tested whether hK5His could inhibit macrophage migration *in vitro*. A migration assay was done using human monocytes isolated from peripheral blood mononuclear cells that were stimulated with GM-CSF to differentiate into CD206$^+$ macrophages (data not shown). The ability of macrophages to migrate through a gelatin matrix was assessed under serum-stimulated conditions, where macrophages were directly exposed to conditioned medium collected from GFP-expressing glioma cells and hK5His-GFP-expressing glioma cells. The results indicate that soluble hK5His decreases the migration potential of human macrophages by ~60% compared with the GFP control ($P = 0.007$, Fig. 5C).

Glioma-targeted hK5His expression suppresses tumor growth and prolongs survival in an experimental orthotopic brain cancer model. To test the efficacy of retrovirally engineered glioma cells secreting hK5His in a clinically relevant proof-of-principle experiment, 10^5 U87-GFP ($n = 5$) and U87-hK5His-GFP cells derived from either a single clone ($n = 5$) and an independently generated polyclonal population ($n = 5$) were implanted intracerebrally in athymic *nu/nu* (nude) mice. Mice were sacrificed 32 days after implantation and brains were removed and processed for H&E staining (Fig. 6A). Tumor volumes from each experimental group were estimated from H&E-stained cryostat sections and calculated as described in Materials and Methods. Consistent with our previous study (28), brain tumors in the GFP control group had extensive growth. In contrast, the U87-hK5His-GFP-implanted mice possessed significantly reduced mean tumor volumes (0.35 ± 0.18 mm^3 for the single clone population and 0.07 ± 0.03 mm^3 for the polyclonal population) compared with the control U87-GFP-implanted (12.23 ± 6.07 mm^3) mice ($P = 0.04$; Fig. 6B).

We did a long-term *in vivo* study, where we evaluated the survival of the therapeutic cohort implanted with U87-hK5His-GFP cells ($n = 15$) and the control U87-GFP-implanted ($n = 10$) mice. Although all control mice succumbed to excessive tumor burden by ~8 weeks, the U87-hK5His-GFP-implanted mice possessed a clear survival advantage with 53% of the mice surviving over 120 days ($P < 0.0001$; Fig. 6C).

Discussion

This present study shows that eukaryotically expressed secreted hK5His protein preserves the prototypical native kringle disulfide bridging conformation deemed essential for the angiostatic activity of plasminogen-derived peptide domains. Indeed, our cysteine
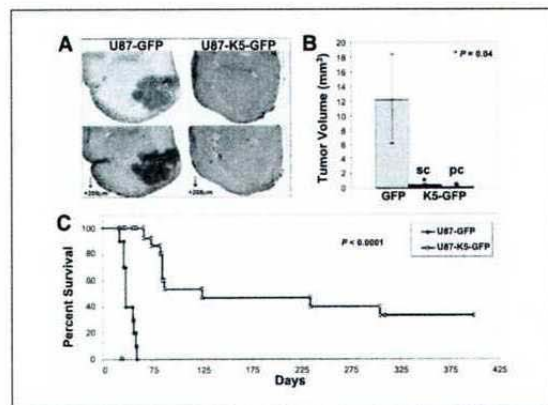
Figure 6. Suppression of intracerebral U87MG glioma growth by soluble hK5His. *A,* H&E-stained brain tissue sections from control U87-GFP implanted mice (*n* = 5) and U87-hK5His-GFP implanted mice (*n* = 5) 32 days after implantation. Representative stains are shown at the same magnification, 40×. *B,* tumor volumes were estimated from postmortem H&E-stained brain sections obtained from mice implanted with U87-GFP, U87-hK5His-GFP single clone (*sc*), and U87-hK5His-GFP polyclonal (*pc*) cells. The experiment was done twice with similar results. *Bars,* SE. Student's *t* test. *C,* Kaplan-Meier long-term survival curve of mice implanted with control U87-GFP (*n* = 10) and U87-hK5His-GFP (*n* = 15) cells. Log-rank statistical test.

bridging pattern data confirms the results of the only other study that characterizes the structure of recombinant K5 domain using NMR technology (29). We have shown that VSV-G-pseudotyped retroviral vectors engineered to express human plasminogen hK5His domain can efficiently gene modify human U87 glioma cells *ex vivo*. We also show that hK5His-engineered U87 cells can secrete biologically functional soluble hK5His protein capable of inhibiting growth factor–stimulated endothelial cell migration *in vitro*.

Moreover, our *in vivo* data in immunodeficient NOD-SCID mice suggests that hK5His secreted by Matrigel-embedded U87 engineered cells acts as a potent antiangiogenic agent by significantly decreasing blood vessel formation as well as a novel antimacrophage agent by significantly preventing the recruitment of host-derived tumor-associated CD45$^+$Mac3$^+$Gr1$^{+/-}$ monocytes/macrophages within the local tumor microenvironment. The involvement of tumor-associated macrophages in angiogenesis and tumor progression is a well-established concept (31–33). Activated macrophages produce tumor necrosis factor-α and IL-1, inducing the production of VEGF and IL-8 in glioma cells, which further attracts and activates macrophages (34). Macrophage infiltration has been closely correlated with neovascularization and observed more frequently in grade 4 glioblastomas than in grade 2 or 3 gliomas (34).

It may be speculated that the potent antiangiogenic properties of soluble K5 mediating a reduction in tumor-associated endothelial cells, as evidenced by the lower surface area occupied by blood vessels in the U87-hK5His-GFP-containing explants, is partially responsible for the decreased infiltration of host-derived macrophages within the tumor area. We also show that soluble hK5His independently reduces macrophage migration *in vitro*, suggesting that the K5 domain can impart a direct inhibitory effect on macrophage motility. To date, the K5 peptide has been consistently characterized as an endothelial cell–specific inhibitor (19, 30) and

Gonzalez-Gronow et al. (35) suggest that K5 mediates its effects by binding to the human voltage-dependent anion channel, which is a receptor present on human endothelial cells. Unlike K5, the mechanism of action of angiostatin has been studied more extensively and its endothelial cell binding sites include the cell surface–associated ATP synthase receptor (36), angiomotin (37), and integrin $\alpha_v\beta_3$ (38). Although angiostatin mediates its inhibitory action primarily on endothelial cells, it has been reported by Moulton et al. (39) that it reduces plaque angiogenesis and atherosclerosis by reducing plaque-associated macrophages. However, Moulton et al. suggest that angiostatin, at doses that reduce endothelial cell sprouting, does not directly inhibit monocytes because it does not inhibit VEGF-induced monocyte migration *in vitro*. Thus, our findings provide novel mechanistic insight and suggest that soluble hK5His protein inhibits two unique cell types most critical for tumor angiogenesis, mediating a dual role as an antiangiogenic agent via its antiendothelial cell properties as well as an antitumor agent by reducing the infiltration of host-derived macrophages within the tumor microenvironment.

We used a clinically relevant orthotopic implantation approach to test whether soluble hK5His could suppress glioma progression after implantation of hK5His-GFP-expressing U87 cells in athymic *nu/nu* mice. Stereotactic implantation procedures are particularly suitable for glioma gene therapy approaches allowing for constant long-lasting transgene expression within the local tumor microenvironment and minimize the risk of toxicity as is often encountered with systemic therapies. Our data successfully shows that soluble hK5His significantly decreases tumor growth by ~97% compared with controls. In doing so, soluble hK5His also promotes long-term survival, with 53% of U87-hK5His-GFP-implanted mice surviving past 120 days. We postulate that upon stereotactic implantation of our *ex vivo* retrovirally engineered hK5His glioma cells, stable integration and sustained expression of the hK5His transgene in target U87 cells provided continuous release of soluble hK5His within the loco-regional tumor microenvironment, resulting in potent suppression of tumor growth. We speculate that tumor-targeted delivery of hK5His via viral vectors such as pseudotyped retrovectors (24) and other gene delivery platforms would lead to similar results.

In summary, we provide compelling evidence that secreted hK5His protein expressed by engineered glioma cells possesses potent antiangiogenic as well as novel antimacrophage properties that block glioma progression and promote survival in an orthotopic experimental brain cancer model. Further studies on the pleiotropic effects of K5 peptide on host-derived angiogenic and macrophage response may offer new avenues of exploration for the development of therapeutic strategies for the treatment of glioma and other loco-regional refractory malignancies such as prostate and ovarian cancer.
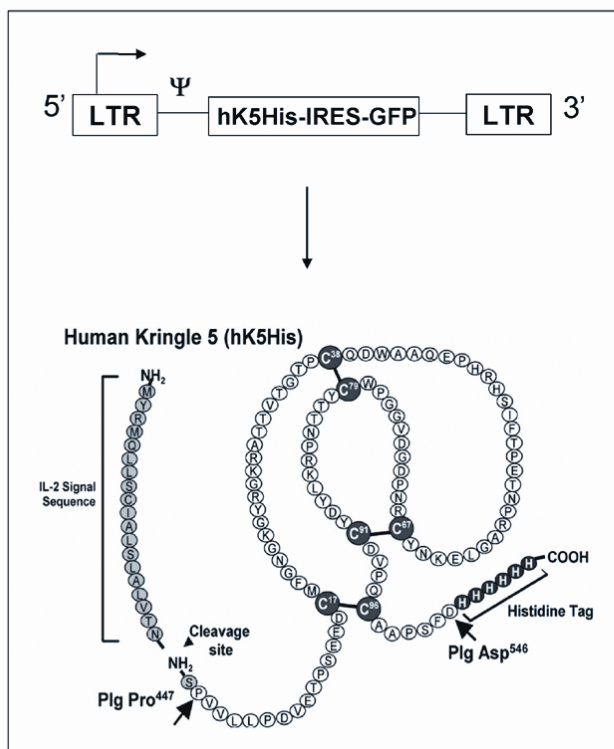
Acknowledgments

References

1. Bello L, Giussani C, Carrabba G, Pluderi M, Costa F, Bikfalvi A. Angiogenesis and invasion in Gliomas. In: Kirsch M, Black PM, editors. Norwell: Kluwer; 2004. p. 263–84.
2. Holland EC. Glioblastoma multiforme: the terminator. Proc Natl Acad Sci U S A 2000;97:6242–4.
3. Black PM. Brain tumor. Part 2. N Engl J Med 1991; 324:1555–64.
4. Folkman J. Tumor angiogenesis: therapeutic implications. N Engl J Med 1971;285:1182–6.
5. Maher EA, Furnari FB, Bachoo RM, et al. Malignant glioma: genetics and biology of a grave matter. Genes Dev 2001;15:1311–33.
6. Puduvalli VK. Inhibition of angiogenesis as a therapeutic strategy against brain tumors. In: Kirsch M, Black PM, editors. Norwell: Kluwer; 2004. p. 307–36.
7. Bello L, Carrabba G, Giussani C, et al. Low-dose chemotherapy combined with an antiangiogenic drug reduces human glioma growth *in vivo*. Cancer Res 2001;61:7501–6.
8. Bello L, Giussani C, Carrabba G, et al. Suppression of malignant glioma recurrence in a newly developed animal model by endogenous inhibitors. Clin Cancer Res 2002;8:3539–48.
9. Gorski DH, Beckett MA, Jaskowiak NT, et al. Blockage of the vascular endothelial growth factor stress response increases the antitumor effects of ionizing radiation. Cancer Res 1999;59:3374–8.
10. Griscelli F, Li H, Cheong C, et al. Combined effects of radiotherapy and angiostatin gene therapy in glioma tumor model. Proc Natl Acad Sci U S A 2000;97: 6698–703.
11. Hwu WJ, Raizer J, Panageas KS, Lis E. Treatment of metastatic melanoma in the brain with temozolomide and thalidomide. Lancet Oncol 2001;2:634–5.
12. Li L, Rojiani A, Siemann DW. Targeting the tumor vasculature with combretastatin A-4 disodium phosphate: effects on radiation therapy. Int J Radiat Oncol Biol Phys 1998;42:899–903.
13. Mauceri HJ, Hanna NN, Beckett MA, et al. Combined effects of angiostatin and ionizing radiation in antitumour therapy. Nature 1998;394:287–91.
14. O'Reilly MS, Holmgren L, Chen C, Folkman J. Angiostatin induces and sustains dormancy of human primary tumors in mice. Nat Med 1996;2:689–92.

15. O'Reilly MS, Boehm T, Shing Y, et al. Endostatin: an endogenous inhibitor of angiogenesis and tumor growth. Cell 1997;88:277–85.
16. Shir A, Levitzki A. Gene therapy for glioblastoma: future perspective for delivery systems and molecular targets. Cell Mol Neurobiol 2001;21:645–56.
17. Kirsch M, Strasser J, Allende R, Bello L, Zhang J, Black PM. Angiostatin suppresses malignant glioma growth *in vivo*. Cancer Res 1998;58:4654–9.
18. O'Reilly MS, Holmgren L, Shing Y, et al. Angiostatin: a novel angiogenesis inhibitor that mediates the suppression of metastases by a Lewis lung carcinoma. Cell 1994;79:315–28.
19. Cao Y, Chen A, An SS, Ji RW, Davidson D, Llinas M. Kringle 5 of plasminogen is a novel inhibitor of endothelial cell growth. J Biol Chem 1997;272:22924–8.
20. Cao Y, Ji RW, Davidson D, et al. Kringle domains of human angiostatin. Characterization of the antiproliferative activity on endothelial cells. J Biol Chem 1996;271:29461–7.
21. Cao R, Wu HL, Veitonmaki N, et al. Suppression of angiogenesis and tumor growth by the inhibitor K1-5 generated by plasmin-mediated proteolysis. Proc Natl Acad Sci U S A 1999;96:5728–33.
22. Ory DS, Neugeboren BA, Mulligan RC. A stable human-derived packaging cell line for production of high titer retrovirus/vesicular stomatitis virus G pseudotypes. Proc Natl Acad Sci U S A 1996;93:11400–6.
23. Ponten J, Macintyre EH. Long term culture of normal and neoplastic human glia. Acta Pathol Microbiol Scand 1968;74:465–86.
24. Galipeau J, Li H, Paquin A, Sicilia F, Karpati G, Nalbantoglu J. Vesicular stomatitis virus G pseudotyped retrovector mediates effective *in vivo* suicide gene delivery in experimental brain cancer. Cancer Res 1999;59:2384–94.
25. Eliopoulos N, Galipeau J. Green fluorescent protein. In: Hicks BW, editor. Totowa: Humana Press Inc.; 2002. p. 353–71.
26. Annabi B, Lachambre MP, Bousquet-Gagnon N, Page M, Gingras D, Beliveau R. Green tea polyphenol (-)-epigallocatechin 3-gallate inhibits MMP-2 secretion and MT1-MMP-driven migration in glioblastoma cells. Biochim Biophys Acta 2002;1542:209–20.
27. Stagg J, Lejeune L, Paquin A, Galipeau J. Marrow stromal cells for interleukin-2 delivery in cancer immunotherapy. Hum Gene Ther 2004;15:597–608.

28. Li H, onso-Vanegas M, Colicos MA, et al. Intracerebral adenovirus-mediated p53 tumor suppressor gene therapy for experimental human glioma. Clin Cancer Res 1999;5:637–42.
29. Chang Y, Mochalkin I, McCance SG, Cheng B, Tulinsky A, Castellino FJ. Structure and ligand binding determinants of the recombinant kringle 5 domain of human plasminogen. Biochemistry 1998;37:3258–71.
30. Ji WR, Barrientos LG, Llinas M, et al. Selective inhibition by kringle 5 of human plasminogen on endothelial cell migration, an important process in angiogenesis. Biochem Biophys Res Commun 1998;247: 414–9.
31. Leek RD, Lewis CE, Whitehouse R, Greenall M, Clarke J, Harris AL. Association of macrophage infiltration with angiogenesis and prognosis in invasive breast carcinoma. Cancer Res 1996;56:4625–9.
32. Richter G, Kruger-Krasagakes S, Hein G, et al. Interleukin 10 transfected into Chinese hamster ovary cells prevents tumor growth and macrophage infiltration. Cancer Res 1993;53:4134–7.
33. Sunderkotter C, Steinbrink K, Goebeler M, Bhardwaj R, Sorg C. Macrophages and angiogenesis. J Leukoc Biol 1994;55:410–22.
34. Nishie A, Ono M, Shono T, et al. Macrophage infiltration and heme oxygenase-1 expression correlate with angiogenesis in human gliomas. Clin Cancer Res 1999;5:1107–13.
35. Gonzalez-Gronow M, Kalfa T, Johnson CE, Gawdi G, Pizzo SV. The voltage-dependent anion channel is a receptor for plasminogen kringle 5 on human endothelial cells. J Biol Chem 2003;278:27312–8.
36. Moser TL, Stack MS, Asplin I, et al. Angiostatin binds ATP synthase on the surface of human endothelial cells. Proc Natl Acad Sci U S A 1999;96:2811–6.
37. Troyanovsky B, Levchenko T, Mansson G, Matvijenko O, Holmgren L. Angiomotin: an angiostatin binding protein that regulates endothelial cell migration and tube formation. J Cell Biol 2001;152:1247–54.
38. Tarui T, Miles LA, Takada Y. Specific interaction of angiostatin with integrin α(v)β(3) in endothelial cells. J Biol Chem 2001;276:39562–8.
39. Moulton KS, Vakili K, Zurakowski D, et al. Inhibition of plaque neovascularization reduces macrophage accumulation and progression of advanced atherosclerosis. Proc Natl Acad Sci U S A 2003;100: 4736–41.
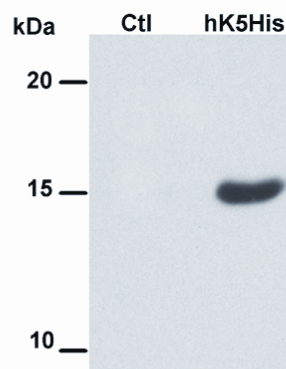
SUPPORTING DATA (unpublished data)

FIGURES

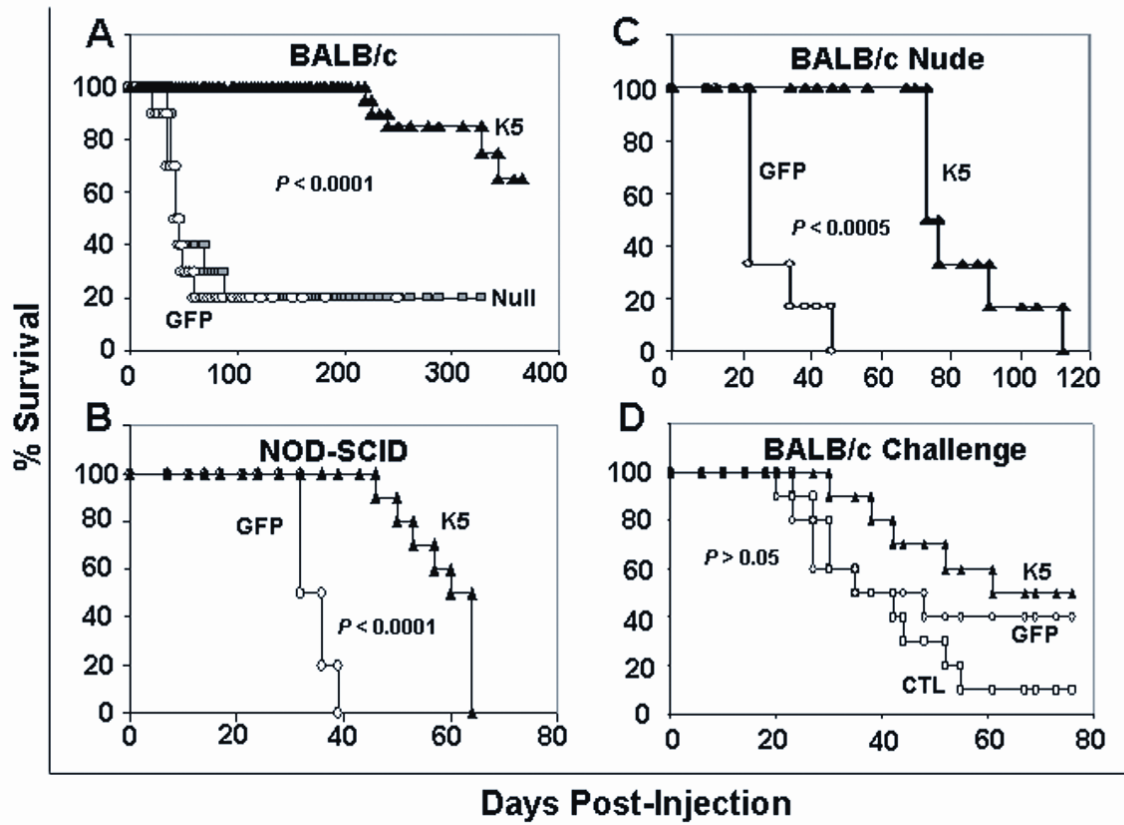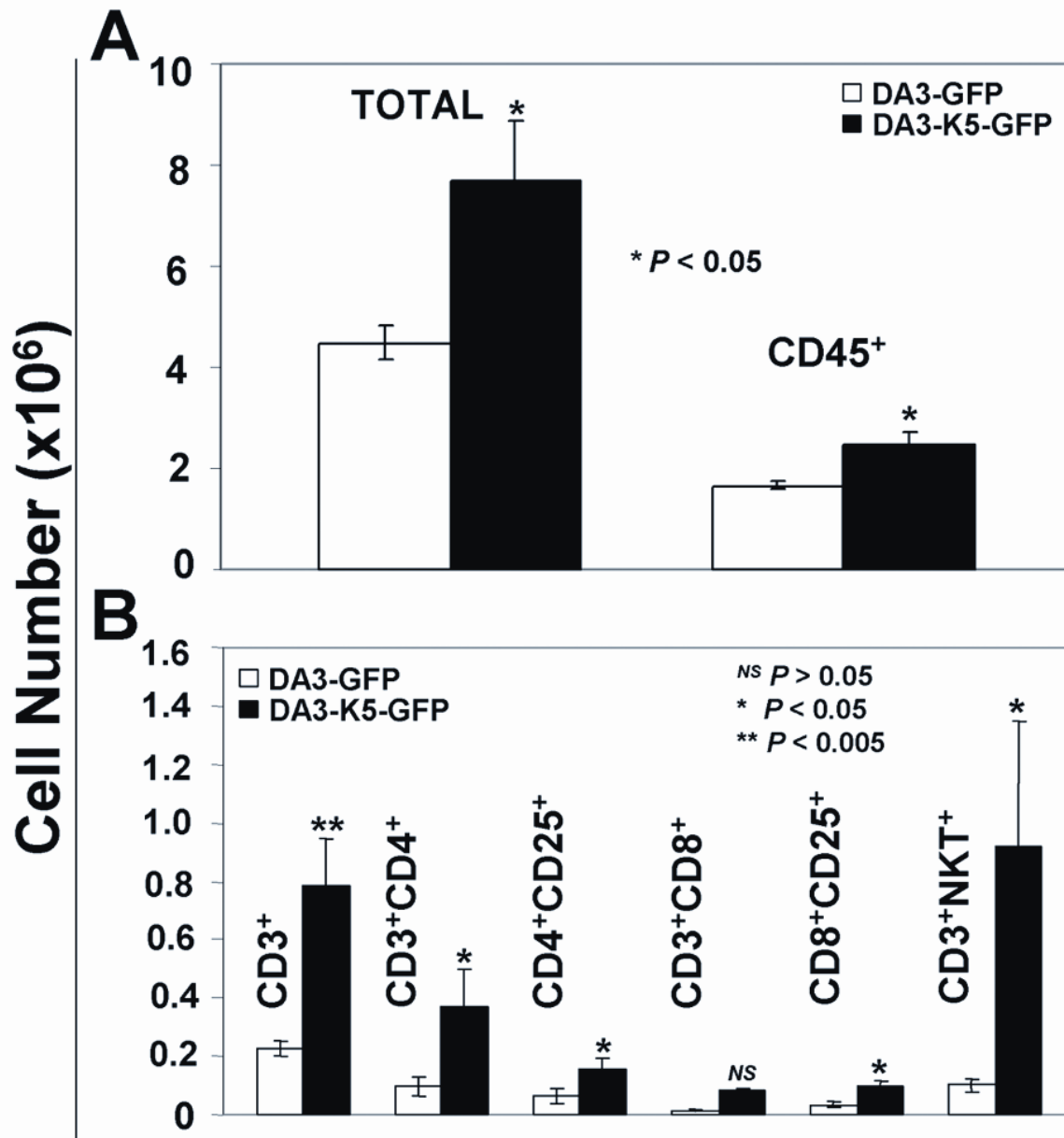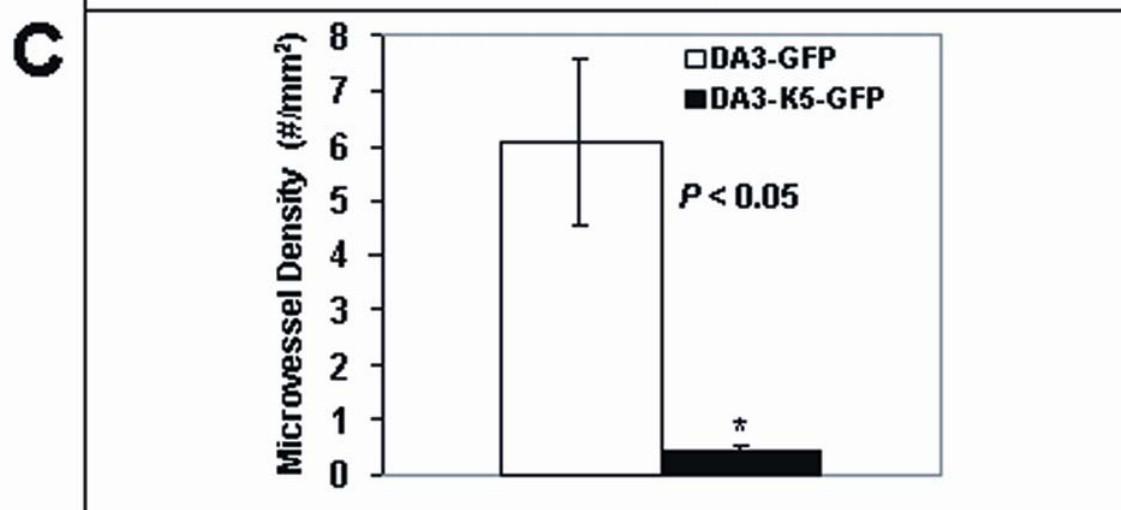S. R. PERRI, Figure 3

A

Isotype **4%**

CD11b **98%**

B

* $P < 0.05$
** $P < 0.0005$

RFU (x10³)

**

**

*

C

CD11b⁺CD64⁺

* $P < 0.05$
** $P < 0.0005$

Expression (%)

**

*

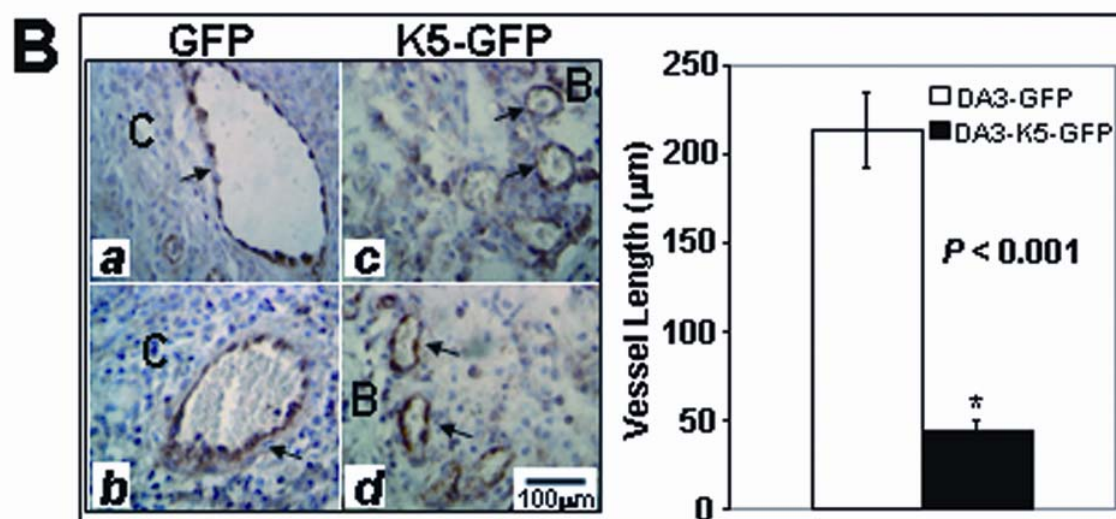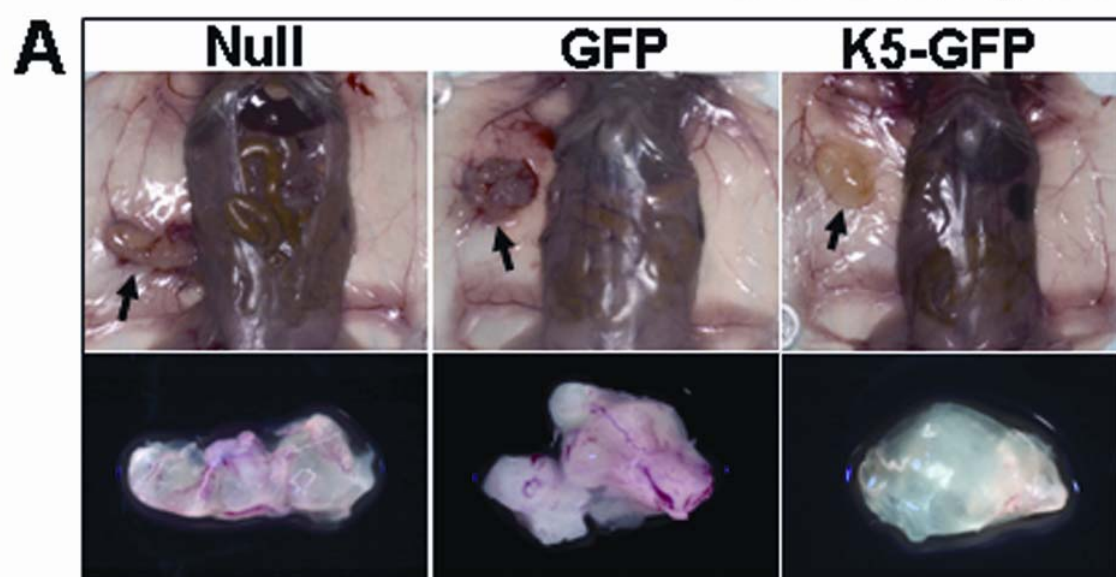**

**
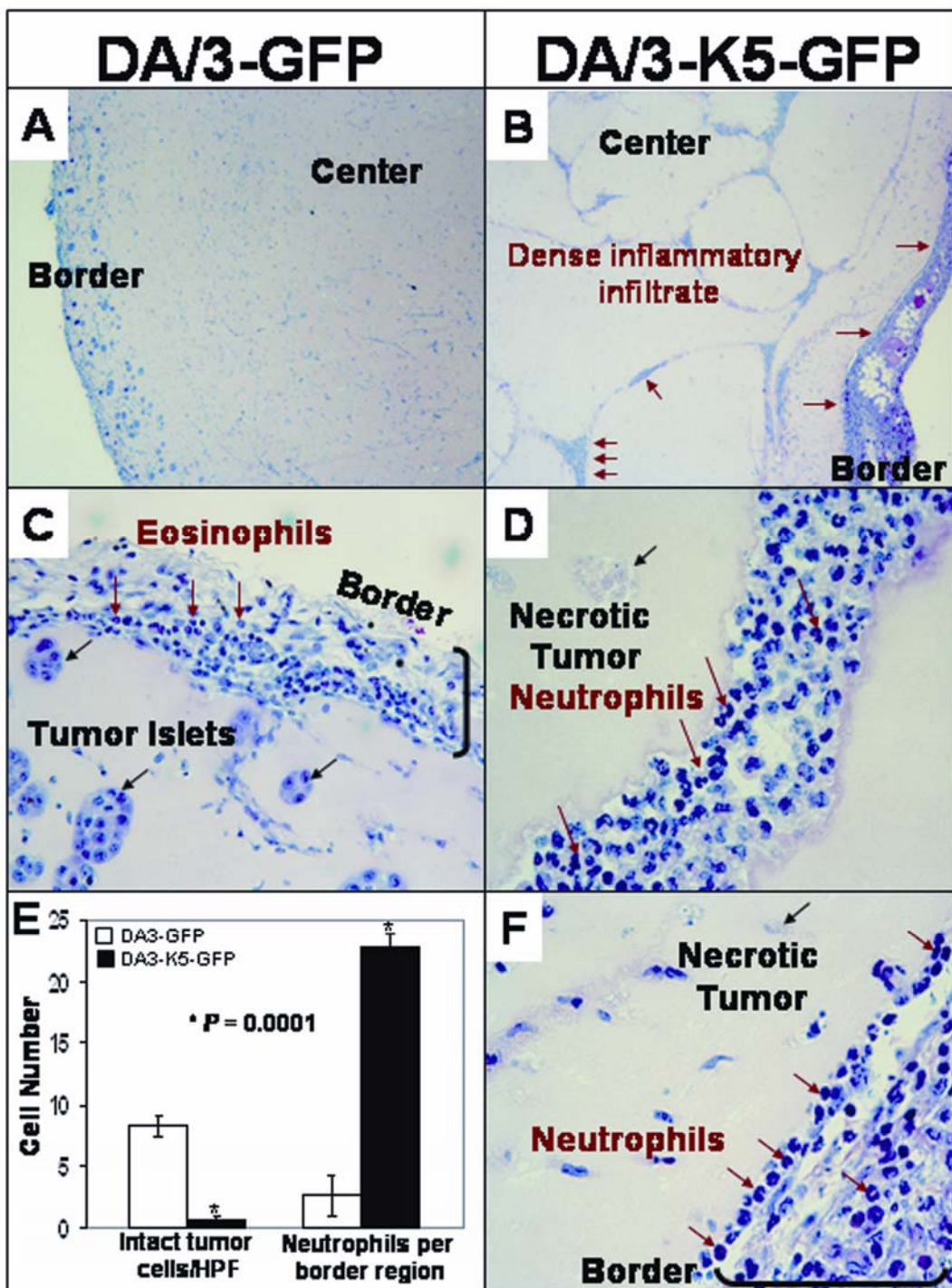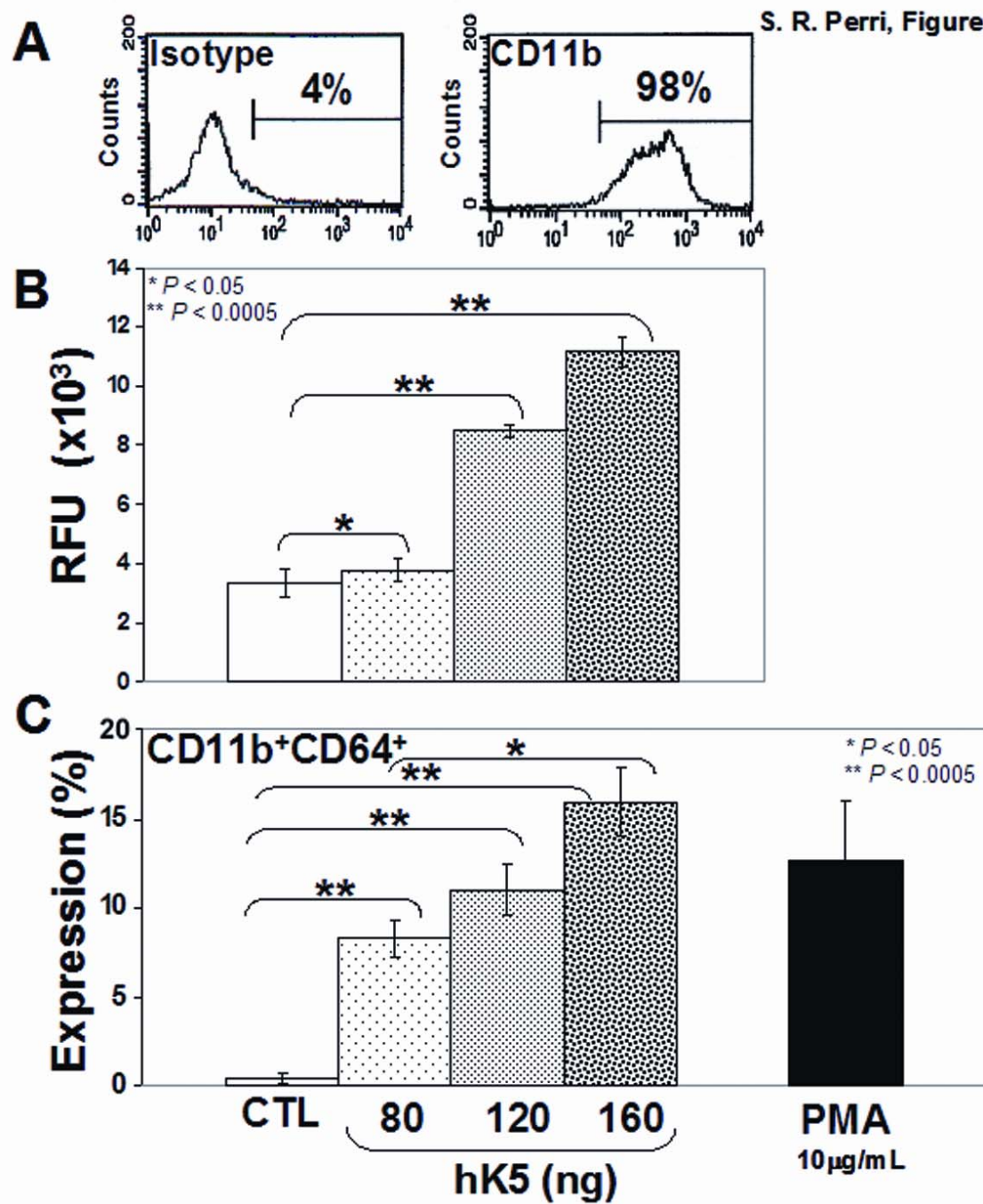
**

CTL   80   120   160   PMA
10μg/mL

hK5 (ng)

S. R. Perri, Figure 6

FIGURE LEGENDS

Figure 1. Development and characterization of hK5His-GFP gene-modified DA/3 cells. *A*, Human kringle 5 (hK5His) retrovector when integrated in DA/3 cells. hK5His consists of the last cryptic fragment of plasminogen (Cys^{462}-Cys^{541}) and is composed of 80 amino acid residues with 3 distinct disulfide bonds. *B*, Anti-His immunoblot analysis reveals functional secretion of hK5His migrating at ~15kDa from retrovirally gene-modified DA/3 cells.

Figure 2. hK5His-GFP-implanted immunocompetent mice survive long-term and modulate the immune system to suppress tumor growth. Kaplan-Meier long-term survival of *A*, immunocompetent Balb/c mice implanted subcutaneously with 10^6 non-gene-modified DA/3 ($n = 10$), GFP-expressing DA/3 ($n = 10$) or hK5His-GFP-expressing DA/3 cells ($n = 10$). The experiment was performed twice with similar results. Kaplan-Meier survival of *B*, immunodeficient NOD-SCID mice and *C*, athymic BALB/c nude mice implanted subcutaneously with 10^6 GFP-expressing DA/3 ($n = 10$, $n = 6$ respectively) and hK5His-GFP-expressing DA/3 cells ($n = 10$, $n = 6$ respectively). *D*, Kaplan-Meier survival of immunocompetent BALB/c mice implanted subcutaneously with irradiated 5 x 10^5 GFP-expressing DA/3 ("GFP", $n = 10$) or hK5His-GFP-expressing DA/3 cells ("K5", $n = 10$) and challenged 14 days later (day 0 on graph) on the opposite flank with 5 x 10^5 non-irradiated GFP-expressing DA/3 cells. BALB/c mice ("CTL", $n = 10$) were independently implanted subcutaneously with 5 x 10^5 non-irradiated GFP-expressing DA/3 cells on the same day as the challenge as a technical control to demonstrate the tumor growth potential. Log-rank statistical test performed for all Kaplan-Meier graphs.

Figure 3. hK5His possesses novel immunostimulatory property. *A, left* Absolute total cell count performed post-collagenase digestion of the explants 3 days post-implantation of 10^6 GFP-expressing DA/3 ($n = 4$) or hK5His-GFP-expressing DA/3 cells ($n = 4$) embedded in Matrigel^{TM}; *right* Absolute number of infiltrated $CD45^+$ hematopoietic cells; *bars*, S.E.M. *B*, Absolute number of infiltrated lymphoid cells: $CD3^+$, $CD3^+CD4^+$, $CD4^+CD25^+$, $CD3^+CD8^+$, $CD8^+CD25^+$, $CD3^+NKT^+$; *bars*, S.E.M. Statistical analysis was performed using the student *t*-test.

Figure 4. hK5His acts as a potent anti-angiogenic agent. *A*, Implant (*arrow*) retrieval 1 week post-implantation of 10^6 Matrigel^{TM} -embedded DA/3, DA/3-GFP or DA/3-hK5His-GFP cells (representative images are shown at the same magnification). *B*, *left panel* Representative images of vWF-positive immunostained blood vessels (*black arrows*) from two different DA/3-GFP-containing (*a, b*) and DA/3-hK5His-GFP-containing (*c, d*) implants; C, center of implant; B, border of implant; magnification 160X; *right panel* The mean vWF-positive vessel length (μm) is plotted for both experimental groups; *bars*, S.E.M. *C*, The microvessel density is plotted as the mean number of vWF-positive blood vessels divided by the mean section surface area (mm^2); *bars*, S.E.M. Statistical analysis was performed using the student *t*-test.

Figure 5. hK5His protein induces dense pericapillary neutrophilic infiltrate. H&E-stained Matrigel explant sections retrieved 3 days post-implantation containing either GFP-expressing DA/3 cells (*A, 2.5X & C*, 20X) or hK5His-GFP-expressing DA/3 cells (*B, 2.5X, D*, 40X *& E*, 40X). *B*, inflammatory infiltrate (*red arrows*) demonstrated, *C*, eosinophils present along the border region (*red arrows*) and tumor islets composed of 6 cells (*black arrows*) are depicted, *D & F*, neutrophils

within the center region as well as within the border capsule region (*red arrows*) and representative examples of necrotic tumors (*black arrows*) are shown. *E*, Quantitative histological analysis representing the number of intact tumor cells per high power field (*left*) and the number of neutrophils per border region (*right*) composed of concentric layers of edematous immature connective tissue; *bars*. S.E.M. Statistical analysis was performed using the student *t*-test.

Figure 6. hK5His protein acts as a neutrophil chemoattractant and promotes activation. *A*, Expression of CD11b cell-surface adhesion marker on isolated PMN; isotype antibody (*left*), test antibody (*right*). *B*, Relative fluorescence units (RFU) of migrated PMN toward either increasing doses of purified hK5His protein (80, 120, 160ng) diluted in OPTI-MEM or OPTI-MEM alone. *C*, Percent expression of $CD11b^+CD64^+$ PMN post-exposure to either increasing doses of purified hK5His protein (80, 120, 160ng) diluted in OPTI-MEM or OPTI-MEM alone or phorbal myristate acetate (PMA, 10µg/mL) as a positive control; *bars*, S.E.M. Statistical analysis was performed using the student *t*-test.